NASA CR70584

IITRI

GPO PRICE $ _____

CFSTI PRICE(S) $ _____

Hard copy (HC) 3.00

Microfiche (MF) .75

ff 653 July 65

FACILITY FORM 602

N66-18320
(ACCESSION NUMBER)

(THRU)

91
(PAGES)

1
(CODE)

CR 70584
(NASA CR OR TMX OR AD NUMBER)

14
(CATEGORY)

IIT Research Institute

Report No. IITRI-U6010-18
(Technical Summary Report)

DESIGN, DEVELOPMENT, AND FABRICATION OF A PORTABLE SPECTROMETER-TYPE MONITOR

George C. Marshall Space Flight Center
National Aeronautics
and Space Administration

IIT RESEARCH INSTITUTE

Report No. IITRI-U6010-18
(Technical Summary Report)

DESIGN, DEVELOPMENT, AND FABRICATION OF A PORTABLE SPECTROMETER-TYPE MONITOR

June 29, 1964, through January 31, 1966

Contract No. NAS8-11723
IITRI Project U6010

Prepared by

E. L. Grove

of

IIT Research Institute
Technology Center
Chicago, Illinois 60616

for

George C. Marshall Space Flight Center
National Aeronautics and Space Administration
Huntsville, Alabama

Copy No. 9

January 21, 1966

IIT RESEARCH INSTITUTE

FOREWORD

This is Report No. IITRI-U6010-18 (Technical Summary Report) on IITRI Project U6010 (formerly IITRI Project C6038), entitled "Design, Development, and Fabrication of a Portable Spectrometer Type Monitor." The work was conducted for the George C. Marshall Space Flight Center, National Aeronautics and Space Administration, Huntsville, Alabama, under Contract No. NAS8-11723. Mr. R. M. Poorman acted as project monitor. This report covers the period from June 29, 1964, through January 31, 1966.

The research on this program was conducted by E. L. Grove, W. A. Loseke, and E. S. Gordon. Additional assistance was given by H. Betz, R. P. Saperstein, H. Bennett, T. Wonder, C. Giello, R. Schultz, R. B. Schwab, and R. F. Lopresti.

Data are recorded in Logbooks C14948, C14956, C15193, C15342, C15608, C15714, C15942, and C16462.

Respectfully submitted,

IIT RESEARCH INSTITUTE

E. L. Grove
Group Leader
Analytical Chemistry Research

Approved by:

Eli S. Freeman
Manager
Physical Chemistry Research

ELG/cs/jab

ABSTRACT

DESIGN, DEVELOPMENT, AND FABRICATION
OF A PORTABLE SPECTROMETER-TYPE MONITOR N66-18320

A small portable spectrometer was designed and fabricated to monitor oxygen and hydrogen as the free gas or as dissociation products in the inert gas shield of the tungsten-inert gas arc welding process. The hydrogen 6562.8 A and the oxygen 7771.9 A lines are the analytical lines, and the argon 8521.4 A line is the internal standard line. These lines were selected because hydrogen 6562.8 A is the only sensitive line for this element in the near-infrared and near-ultraviolet regions and the oxygen 7771 A triplet is the most sensitive near hydrogen. The argon 8521.4 A line was selected because it has similar characteristics to argon 8408.6 A and is a single line with no spectral interference. Because of design parameters, spectral lines with no other closely adjacent lines were required.

The fixed Eagle mount was chosen because of its simplicity. It has only three optical components: the entrance slit, the collimating diffraction grating, and the camera (exit slits and photomultiplier tubes). A concave grating with a 60-cm focal length and 610 grooves/mm was blazed in the second order. The grating face is 76 x 50 mm and has a reciprocal dispersion of 12 A/mm at 6562 A and 10 A/mm at 8524 A. The theoretical resolving power is 90,000. This instrument resolves the oxygen 7771 A triplet and has an optical speed of approximately f/8.

A fiber optic bundle is used to transmit the light from the arc to the spectrometer, since the arc does not necessarily stay in a fixed plane because of work metal warpage and the use of constant arc-length welding heads. One end of the fiber optic bundle serves as the entrance slit and the other as the limiting aperture. A special probe mounted on the side arm holds a focusing lens with the optical axis 15° to the work metal and the three-dimensional stage diaphragm-aperture mount. The focusing lens gives a 3x magnification of the arc on the 1-mm limiting aperture, so that the very short arcs used in aluminum welding can be monitored. The 1-mm entrance slit is used to compensate to some degree for the light loss in the fiber optic bundle. This wide entrance slit can be used because there are no lines that produce spectral interference.

The varying level of blackbody radiation entering the spectrometer was a serious problem. This was solved by using a rotating optical wedge that causes the emission line to oscillate across the exit slit. This oscillation effectively produces an AC signal above the DC current of the stray blackbody radiation. By using two light-tight compartments, photomultiplier tube changes and exit slit adjustments can be made without disturbing optical alignment.

The solid-state readout system is unique since it is effectively an instantaneous direct-ratio system and not an integration-with-time system. Therefore it is very sensitive. The ratio system relates the analytical to internal standard

response readout and is made possible by the use of the Devar ratio computer in each analytical channel. The ratio is recorded on Rustrak model 88 recorders. The electronics also provides outlets for oscilloscope monitoring of the waveform to establish proper optical alignment of the exit slits.

TABLE OF CONTENTS

LIST OF FIGURES AND TABLES

LIST OF FIGURES AND TABLES (cont.)

DESIGN, DEVELOPMENT, AND FABRICATION OF A PORTABLE SPECTROMETER-TYPE MONITOR

I. SCOPE OF THE PROGRAM

The objective of this program was (1) to study the additional parameters involved in the spectral monitoring of atmospheric contaminants in the tungsten inert gas welding process and (2) to design and construct a compact portable multichannel spectrometer to monitor atmospheric contaminants in inert gas shields.

II. EXPERIMENTAL STUDIES OF SPECTRAL PARAMETERS

A. Spectral and Optical Considerations

1. Equipment and Materials

In order to study the parameters necessary for the design of the portable spectrometer, additional experiments with welding arcs were necessary. Equipment included a variable-speed Linde side-beam carriage and a heavy clampdown fixture mounted on a 10-ft side beam. The beam was held by two 4-in.-diameter steel columns bolted to the floor. The speed of the side beam could be varied from 1 to 120 in./min. The clamp-down fixture was designed to hold plates larger than 18 x 36 in. An Airco model M60-B TIG torch was mounted horizontally

in front of the side-beam fixture on a stationary column. An optical bench support was designed and mounted on this same post. The optical bench and the accessory optics were mounted at right angles to the side beam carriage and spectrograph. The light energy was transmitted from the welding arc to the spectrograph by means of two mirrors and a lens system. By removing one mirror, the spectrograph could be used occasionally for other purposes. Alignment of this system was found to be more critical than expected. The initial experimental layout is shown in Figure 1.

Two aluminum alloys were used during this study, 2219-T87 (9 x 36 x 1/4 in.) and 2024 (18 x 36 x 1 in.). Because of the excessive warping of the 1/4-in.-thick plates from the heat during a welding pass, the 1-in. plates were used for most of these studies. Since these plates still warped too much when using the fixed torch to maintain arc length tolerance, it was replaced with an Airco Automatic Head model HMH-D welding unit. The Brush Recorder Mark II was used to measure voltage drop. Later these readings were checked against a calibrated RCA Senior Voltohmist.

The constant arc length head followed the warping of the metal plate and thus did not remain optically aligned. To overcome this problem, the system on the optical bench was changed and the light was brought to the lens system with a fiber optic bundle. This arrangement is shown in Figure 2.

Figure 1

THE INITIAL EXPERIMENTAL LAYOUT

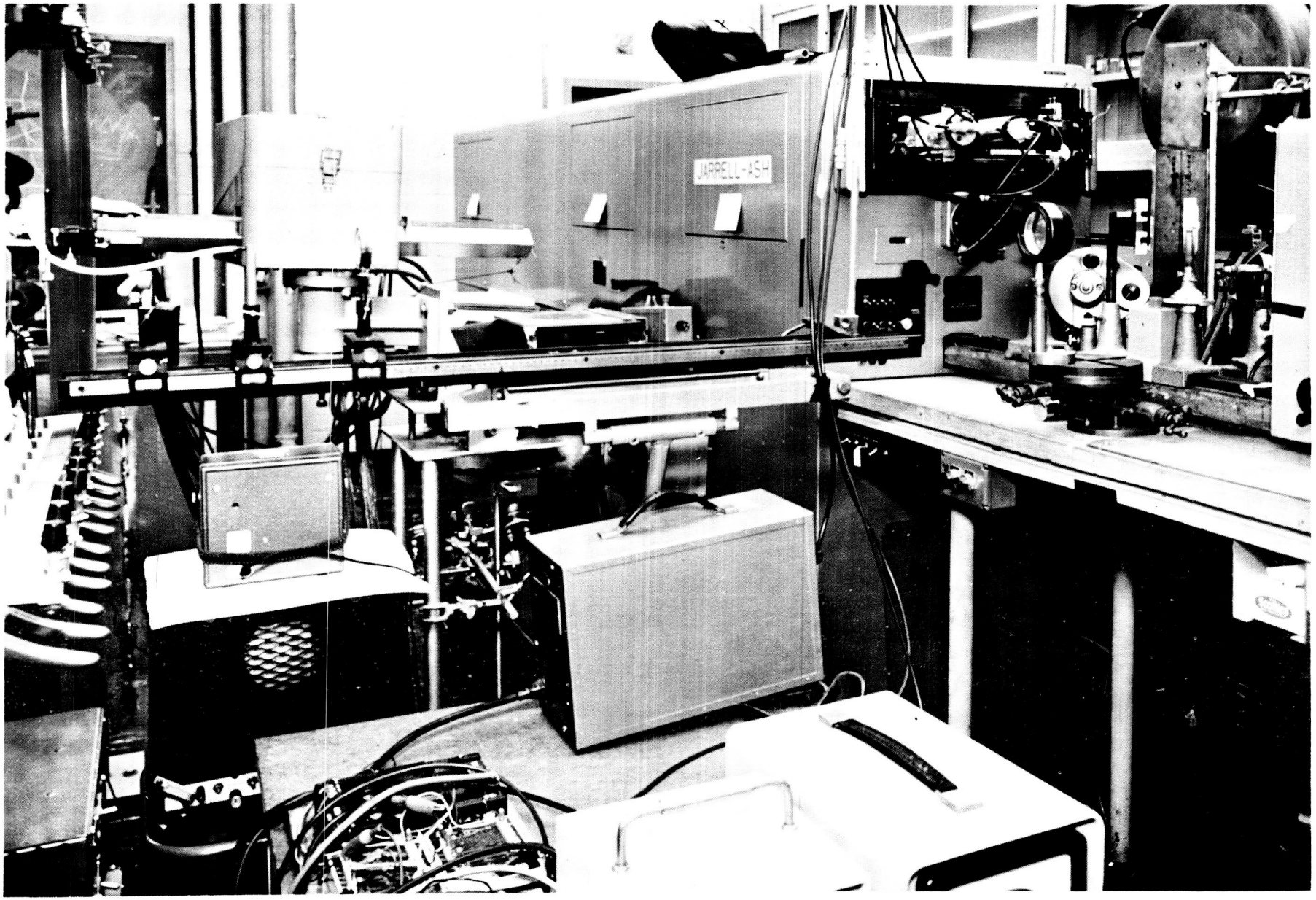

Figure 2

EXPERIMENTAL LAYOUT WITH OPTICS MODIFICATIONS

The end of the fiber optic bundle, which serves as the limiting aperture, was clamped in an aluminum block. This block acted as a diaphragm on which the position of the electrode tip and work metal could be observed. The diaphragm block was mounted on a three-dimensional stage assembled from two microscope stages, thus permitting the positioning and focusing of any portion of the arc on the aperture. A single focusing lens was used. The effective aperture of the lens was 16.5 mm, and it was positioned to accept an 11° solid angle of light. This lens has a 39-mm focal length and was positioned 76 mm from the electrode and 83.5 mm from the aperture, so that its magnification was approximately 1.1. The lens holder and diaphragm unit were mounted on a 1/4-in. aluminum plate, which in turn was mounted on the casting that holds the torch head. Thus the distance from the electrode to the lens is fixed, and the optical axis forms an 11° angle with the work metal. This casting required considerable machine work to prepare a plane surface parallel to the electrode. A small jig was used to position the electrode in proper alignment with the optical axis. The details of the mount are shown in Figures 3 and 4.

The spectrograph was the Jarrell-Ash 3.4-meter Ebert mount instrument, model JA-7102, with a 15,000 line/in. plane grating blazed for 4000 A in the first order. The Jarrell-Ash

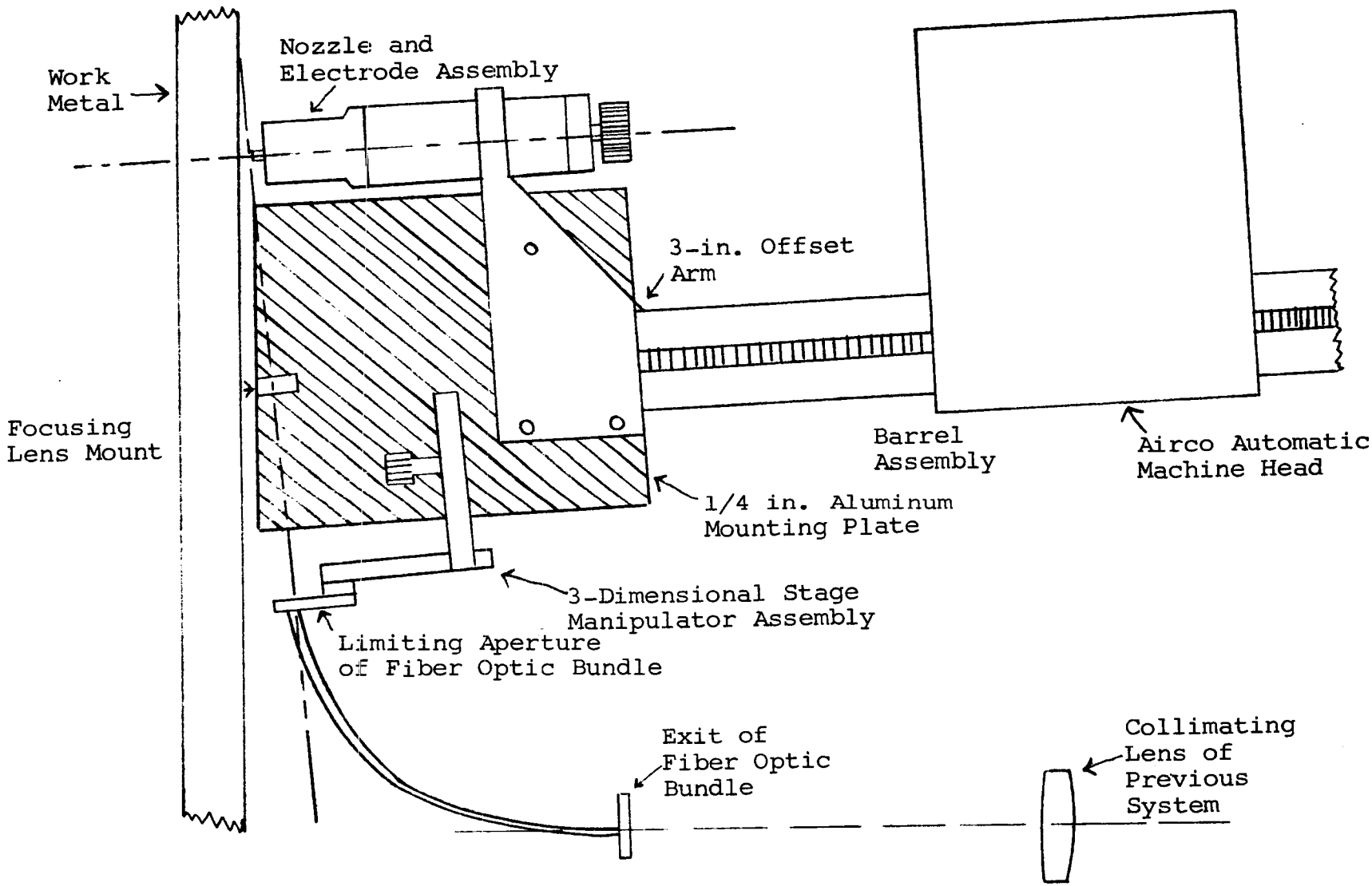

Figure 3

OPTICAL MOUNT WITH HELIWELD TORCH HEAD

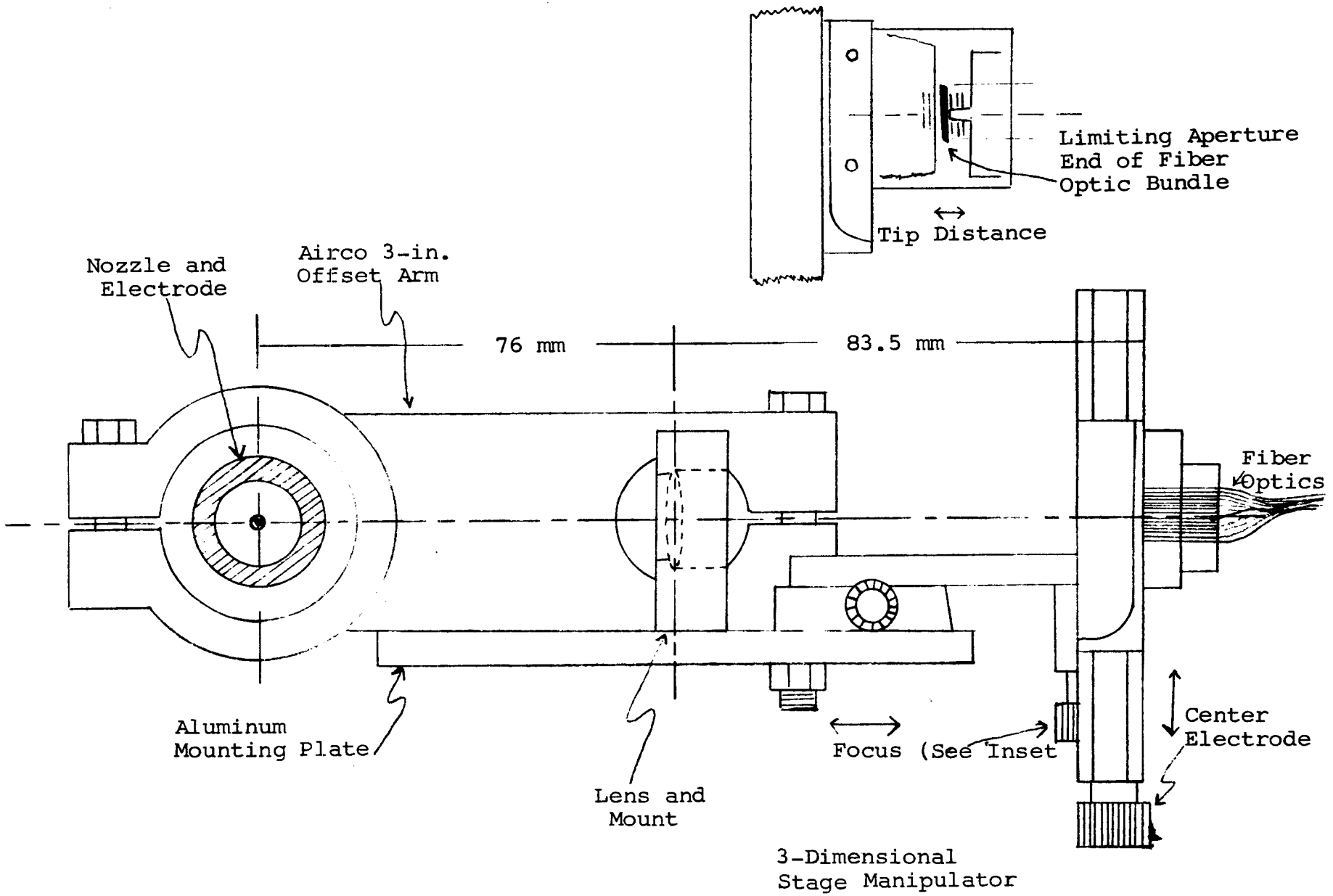

Figure 4

ARRANGEMENT OF SOURCE, CONDENSING LENS, AND FIBER OPTIC APERTURE

comparator microphotometer, model 2100, was used for densitometric measurements. The power source was the Miller model 360P AC-DC welding power unit.

Photomultiplier response data were needed for electronic readout design studies. A plate was designed to support the required end-on type phototubes and was mounted in the plate holder of the spectrograph. Two S-1 response photomultiplier tubes were mounted, one tube sensing an analytical line and the other the internal standard line. A Northeast high-voltage power supply was used to supply voltage to the photomultiplier tubes, and two electronic microvoltmeters were used for readout. A Sanborn model 67-1200 four-channel recorder was used to record some measurements. This unit records the response of each photomultiplier tube directly and the ratio output from the Devar ratio computer.

2. Internal Standard Studies

a. Nondispersed Light

At the beginning of the program we were expecting the welding research group at NASA, Huntsville, to use an argon-helium mixture. For this reason we planned to use an argon emission line as the internal standard line. In previous work we studied several lines, including 7147.5, 7891.1, 7272.9,[1]

[1] E. L. Grove, V. R. Raziunas, W. A. Loseke, and B. K. Davis, "Spectrographic Monitoring of Inert Gas Shields for Atmospheric Contaminants," Welding J., 29, 282, 1964.

7384.0, and 8264.5 A,[2] all of which are in the 13.3-eV excitation potential range.

The decision to use helium as the shield gas created a problem since this element has only three emission lines: 6678.15 A, 2307 eV; 7065.19 A, 22.71 eV; and 7284.35 A, 22.91 eV. These excitation potentials are not compatible with those for oxygen (10.73 eV), hydrogen (12.09 eV), and nitrogen (13.7 eV). The excitation potential of the internal standard line should be as near as possible to that of the analytical lines, so that the internal standard line does not vary if there is an appreciable increase in one or all of the elements of analytical interest.

Since a beam of nondispersed light taken from behind the slit by means of a beam splitter is used as the internal standard in various methods of spectroscopic analysis, this appeared promising. It would save carrying a small quantity of argon and the use of a bleed system.

The output signals from the nondispersed light were quite erratic when the arc length or surface conditions appeared to vary. Even under conditions of apparently uniform surface and nearly constant arc length with the 1 in.-thick 2024 alloy as the work metal, the signal for nondispersed

[2] W. A. Loseke and E. L. Grove, "Analysis of Gaseous Fluorine and Chlorine Compounds by Use of the Stallwood Jet-D.C. Arc," Third National Meeting, Society of Applied Spectroscopy, Sept. 1964.

light was quite unstable, while the signal from an analytical line was quite stable. The recordings taken with a tungsten-to-tungsten low-current arc and with the tungsten-to-plate welding arcs indicated that the changes in the phototube output from the nondispersed light were completely out of proportion with those from the analytical channel. Slight variations in current for plate weld passes resulted in quite large changes in the nondispersed light output. When a low-current tungsten-to-tungsten arc was used, a change from 10 to 20 amp produced a change up to 3.4/1 for the internal standard output and only up to 1.4/1 for the analytical line output with a given level of oxygen. This represents an error of 240%.

The effect of arc length, which is reflected in current and voltage changes, was evaluated from both the output from nondispersed light and dispersed light, i.e., different atomic lines. The 1-in. plate of 2024 alloy was shimmed in order to have a 0.155-in. change for the 36 in. of carriage travel. The initial gap was 0.060 in., and the final gap was 0.215 in. Readings were taken at approximately 6-in. intervals. The results for helium and for helium plus other gas concentrations are summarized in Figure 5. The effect of increasing arc length on three atomic lines is summarized in Figure 6. The nondispersed light varied by approximately 34%, while the intensity of the spectral radiation decreased

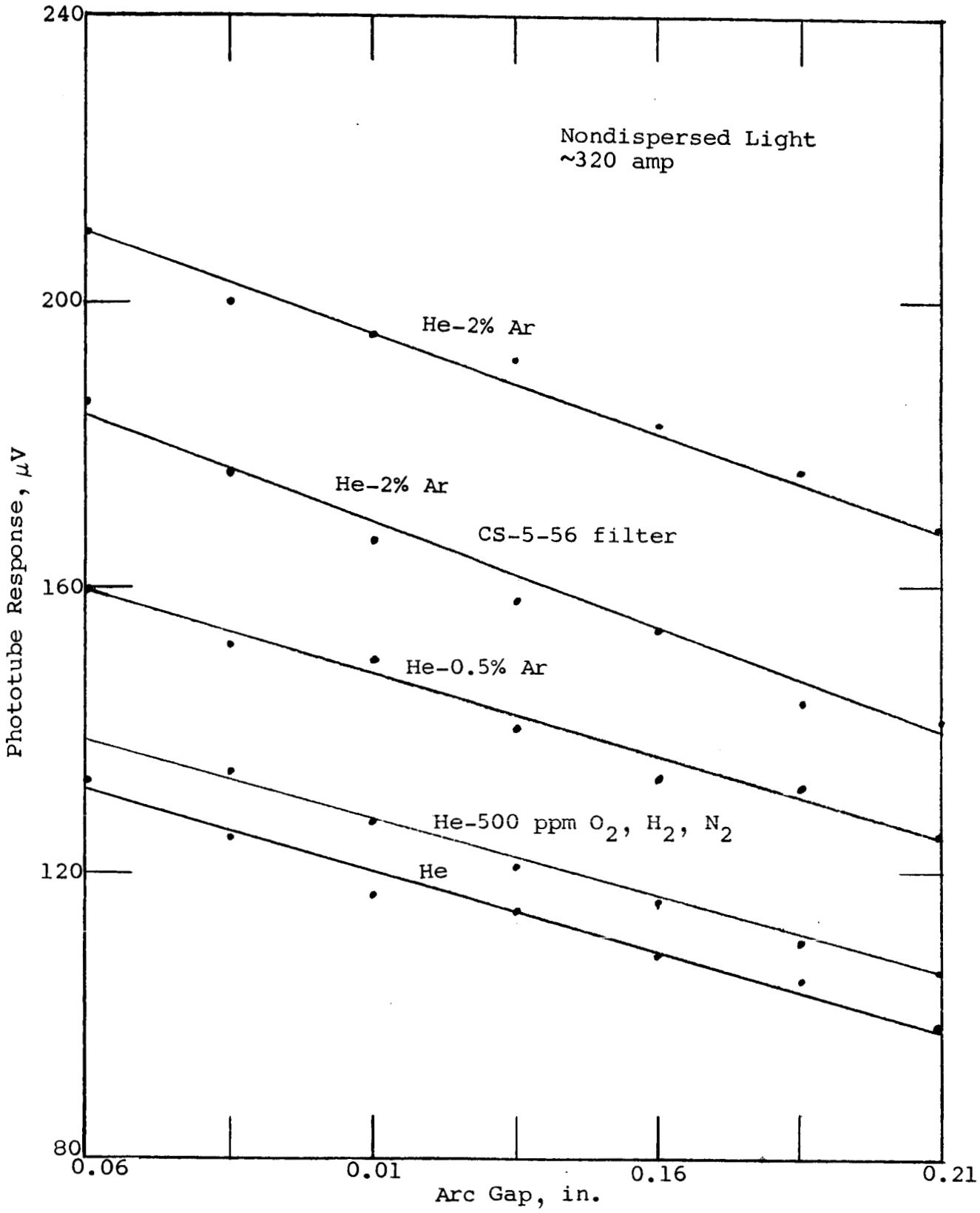

Figure 5

EFFECT OF ARC LENGTH ON NONDISPERSED RADIATION INTENSITY

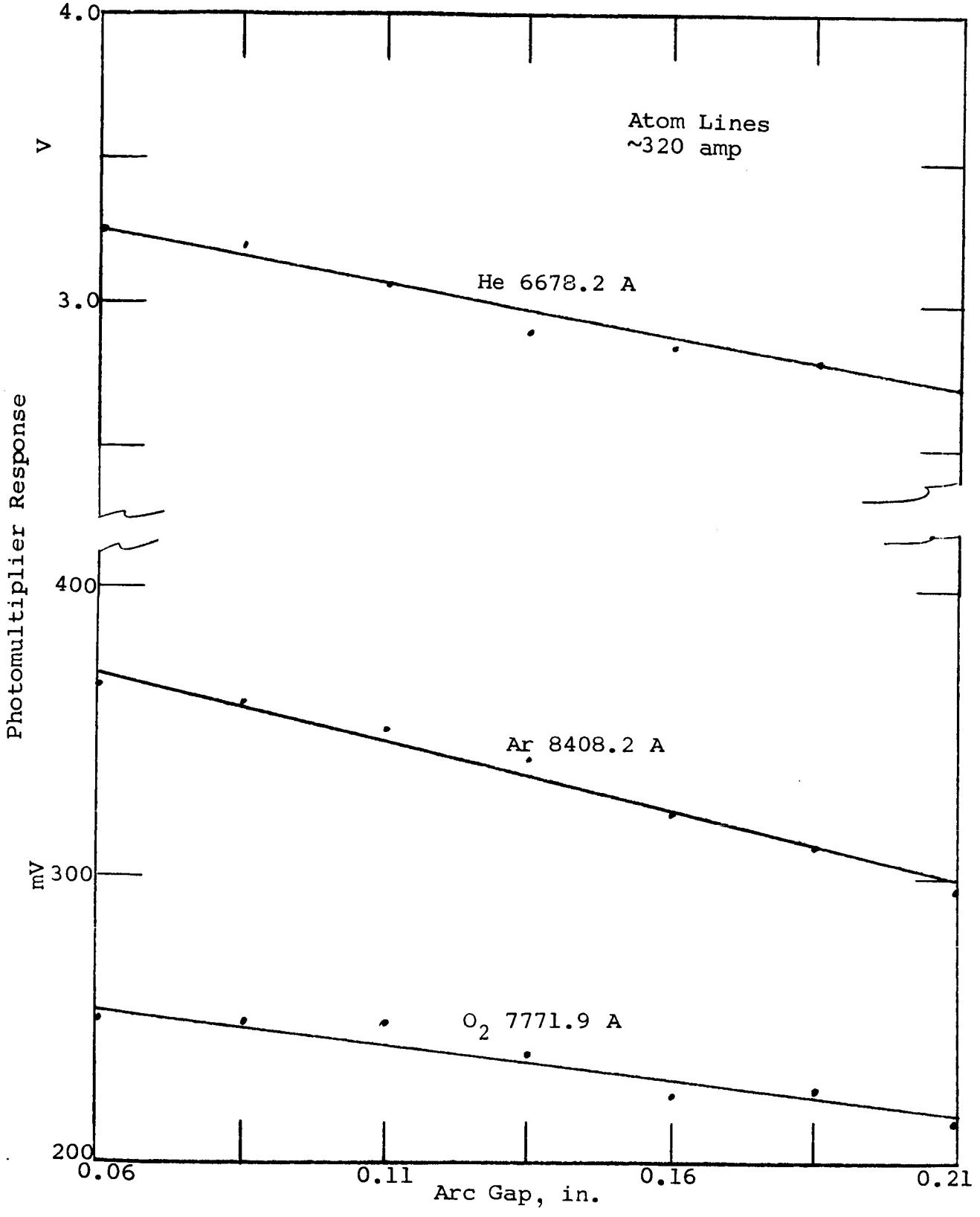

Figure 6

EFFECT OF ARC LENGTH ON LINE RADIATION INTENSITY

by only 14%. In all these experiments the limiting aperture was focused on the same region at a constant distance from the tungsten cathode.

Although nondispersed light is used as the internal standard in conventional analytical emission spectroscopy, it cannot be applied in this situation. The explanation for this lies in the nature of the light in the 2200- to 4400-A region and the 6400- to 8300-A region. Light in a spectral region is essentially made up of the lines and band components of the materials producing the light.

The pure helium arc produced the lowest output from the phototube monitoring the nondispersed light (Figure 5), and the addition of any other component(s) increased the phototube response, even though the temperature of the arc was actually slightly decreased. The arc is being partially carried by species with lower excitation potentials, as shown by the decrease in the intensity of the helium lines. This intensity continues to decrease as the concentration of gases such as argon, oxygen, hydrogen, etc. is increased. The addition of 500 ppm of oxygen, nitrogen, and hydrogen to the helium with 2% argon produced a very small additional increase in phototube response, but it was not sufficient to be illustrated in Figure 5.

A photograph of the light from the helium arc, which is essentially composed of three emission lines, is shown in

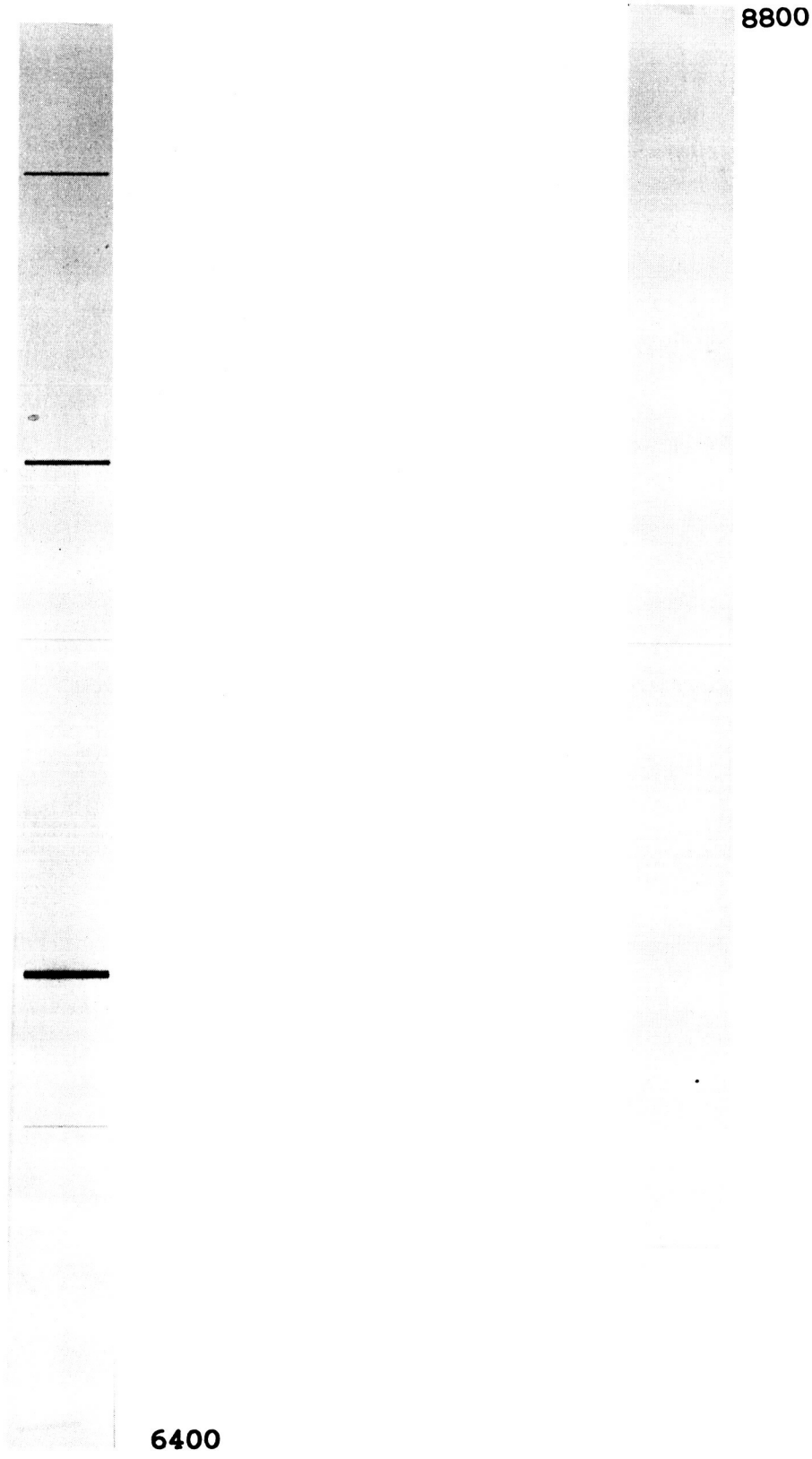

Figure 7

HELIUM SPECTRA

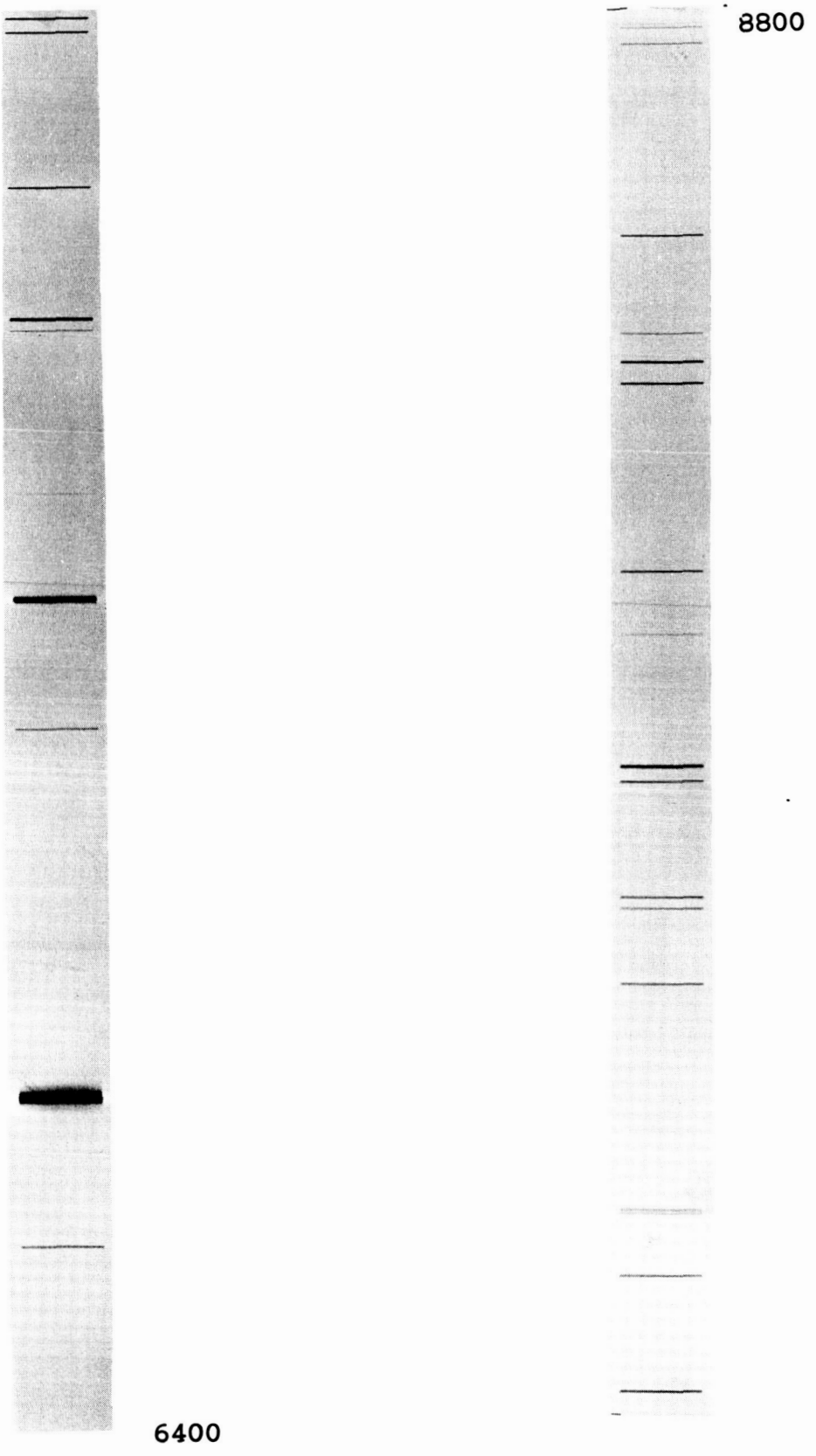

Figure 8

HELIUM-2% ARGON SPECTRA

Figure 7. The addition of another component such as argon produces a spectrum with many more lines (Figure 8), and the signal from nondispersed light is increased, as illustrated in Figure 5. The large increase in response for long arcs could be due to poor shielding; thus air and work metal species became abundant in the arcs.

Most elements have relatively complex spectra in the near-ultraviolet region. For this reason, the very small additional light from the lines of an added internal standard or stray impurities have little effect on the light energy from an already complex spectrum. Therefore the monitoring of the normal or nondispersed light as the internal standard is possible for conventional analytical emission spectroscopy but not for high-current helium arcs.

b. Dispersed Radiation

Areas of dispersed radiation, i.e., areas containing no emission lines (background), were briefly considered by using a 50-μ slit in the spectrograph. With the arc length and the surface condition as constant as possible, the background level was relatively stable for the helium arc at a given concentration of the atmospheric contaminants (Figure 9). However, as atmospheric contaminant was added, a progressive change occurred (Figure 10). This represents a change of 54% with the addition of 300 ppm of atmospheric contaminant, which is much too great for use as a reference. The parallel lines in

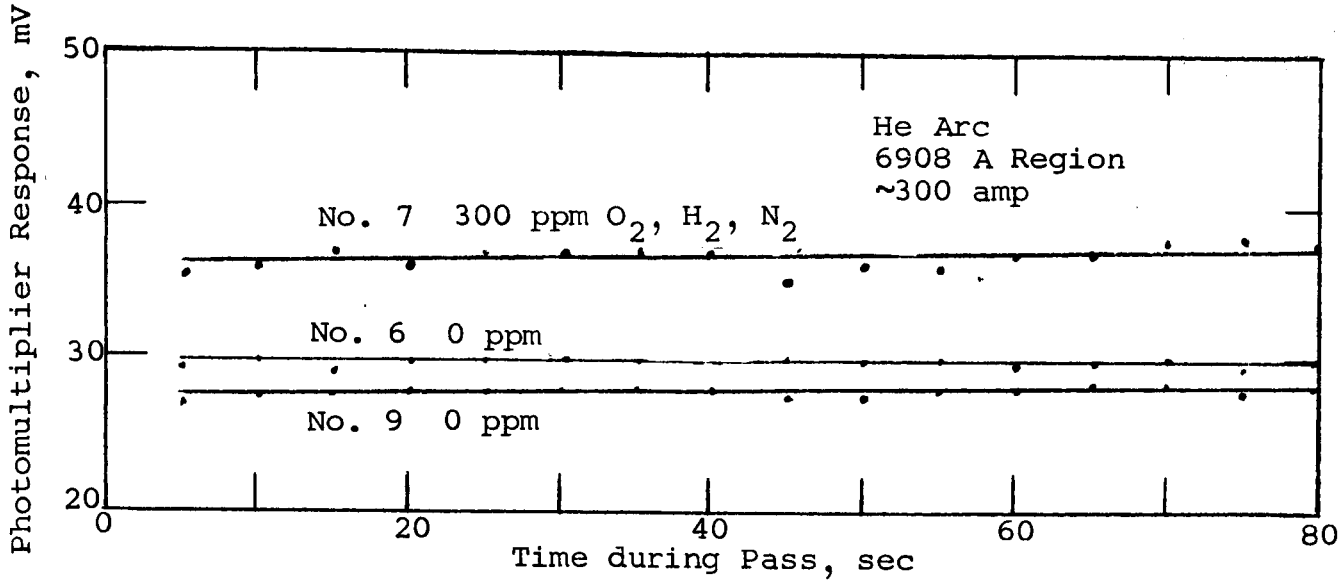

Figure 9

VARIATION IN BACKGROUND DURING WELD PASS

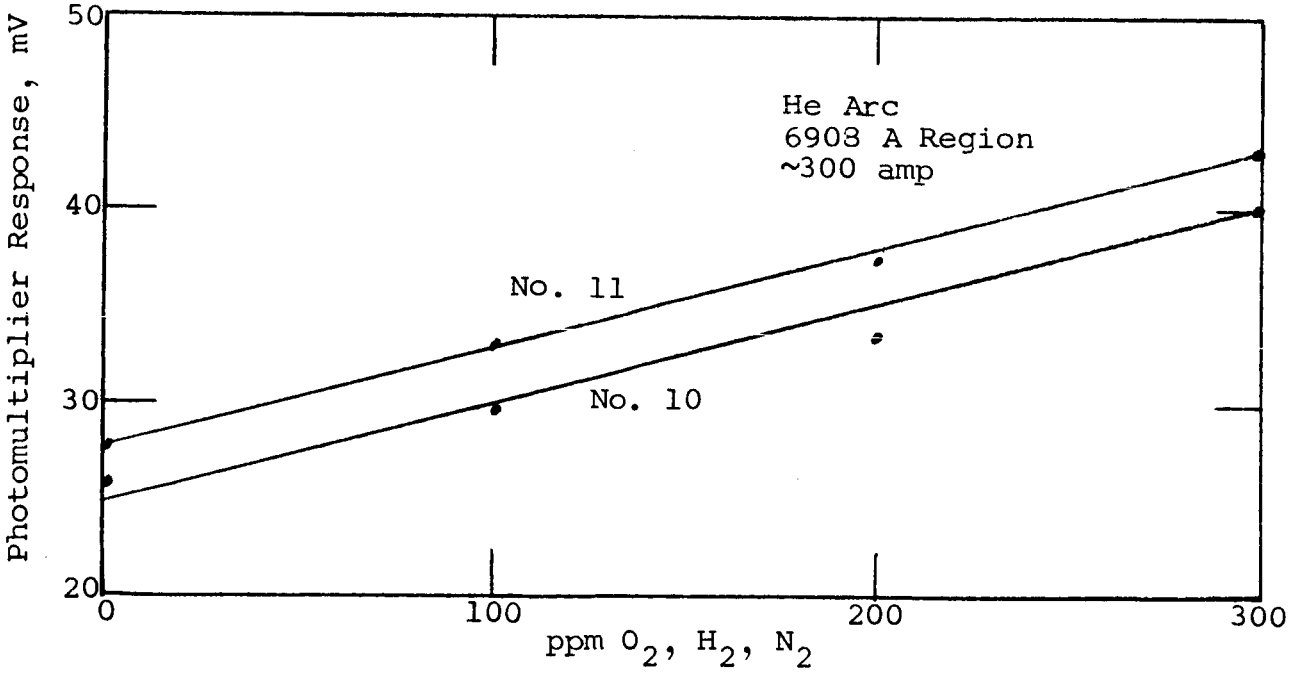

Figure 10

CHANGE IN BACKGROUND WITH ADDITION OF CONTAMINANT

Figures 9 and 10 for the same concentrations represent the difference in readout response caused by very small differences in physical parameters, such as arc length, electrode tip configuration, etc.

c. Evaluation of Argon Lines

The response of three argon lines, 6965, 7384, and 8408 A, and the adjacent backgrounds were measured in a helium-0.5% argon shield gas. The 8408 A line had a much better signal-to-background ratio than either the 6965 or the 7384 A line. Not only was the 8408 A line the strongest, but the intensity of its background was 1/3 and 1/2 that of the 6965 and 7384 A lines, respectively. The signal from these lines under various conditions was much more stable than that of the nondispersed light or background. The effect of increasing concentrations of hydrogen and oxygen on specific argon and helium lines is shown in Figure 11. There is some change in the intensity of the argon line since the excitation potential for argon, 13.09 eV, is less than that for hydrogen, 12.09 eV, and for oxygen, 10.73 eV. Oxygen has a slightly greater effect because of its lower excitation potential. The rather large effect of hydrogen on the 6678 A line, 23.07 eV, for helium illustrates why helium lines are not sutiable for the internal standard. The response from increasing quantities of argon in helium was essentially a straight line (Figure 11). The line was argon 8408 A.

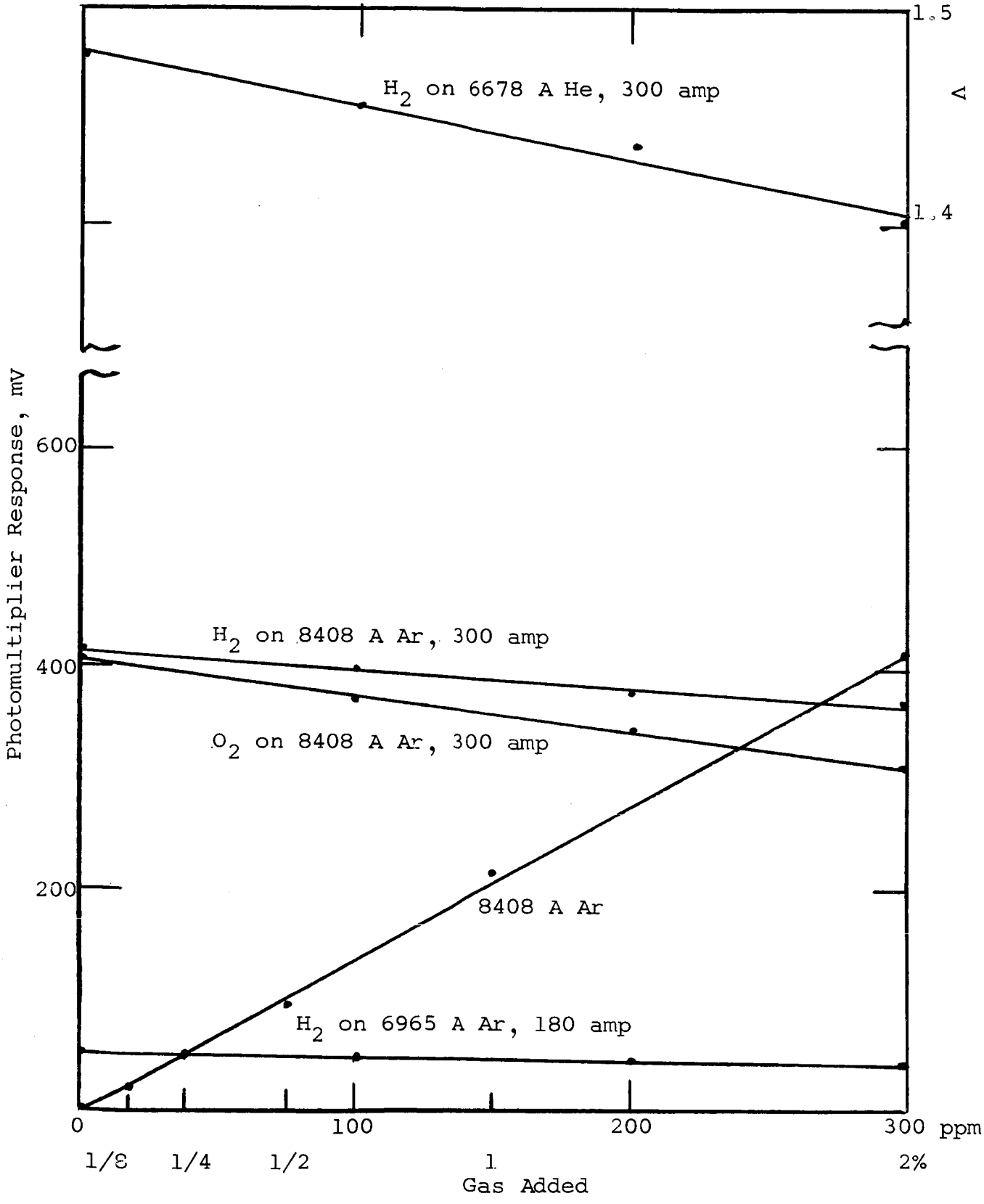

Figure 11

RESPONSE OF POSSIBLE INTERNAL STANDARD LINES

3. Analytical Line Response

The response for the 6562 A hydrogen and 7771 A oxygen lines are linear in the range 0 to 300 ppm (Figure 12). The direct response at 180 amp is less than that at 300 amp; this is to be expected. The source of hydrogen, whether hydrogen gas or a mixture of gases, had no noticeable effect on its response. When a blank was repassed over a bead that had been prepared with increasing levels of hydrogen, there was a small increase in the response; thus entrapped hydrogen must have been entering the arc and being excited (Figure 12). By using a constant quantity of oxygen, the photomultiplier response, when focused on the 7771 A triplet, essentially did not change when the argon in helium was varied from 0 to 2%. This concentration of argon is satisfactory in this range. At this point, as at other times, it was difficult to reproduce direct readings because of slight differences in arc parameters for each pass.

4. Position of Electrode Tip

Since the relative position of the electrode tip with respect to its position to the limiting aperture appeared to significantly affect the photomultiplier responses for the gases, this was briefly examined. A 2x image magnification with a 1-1/4 mm limiting aperture was used to determine the effect of imaging the electrode 0.2, 0.5, and 1.0 mm from the

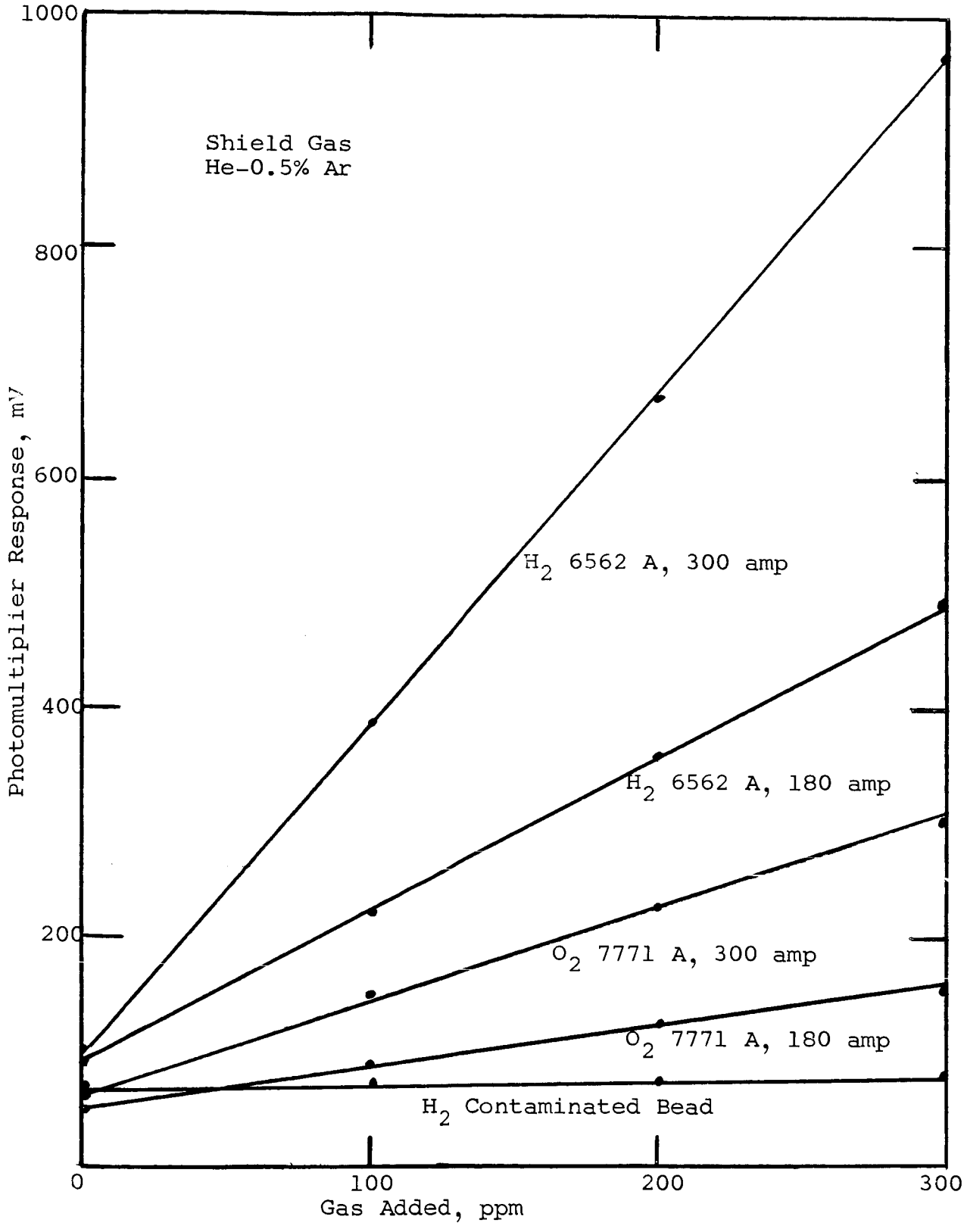

Figure 12

DIRECT RESPONSE OF HYDROGEN AND OXYGEN

aperture edge (Figure 13). The portions of the arc closest to the electrode tip have the greatest abundance of excited species, as indicated by the sensitivity for oxygen at an electrode tip distance of 0.2 mm. This indicates that the position of the arc on the aperture, to the electrode tip from the edge of the limiting aperture must be closely maintained. Thus a small jig was prepared to maintain the electrode tip in a constant position. This jig was used with the assembly shown in Figure 3.

5. Calibration Curve Studies

After the various parameters that affect excitation of the individual gases had been studied, the calibration curves based on the ratio of the intensities of oxygen and hydrogen to that of argon were studied. A family of curves in which 0.125 to 2% argon was used as the internal standard was prepared for oxygen and hydrogen in the 100- to 500-ppm range by the photographic densitometry method. The curves were reasonably parallel, and the precision of the six points in forming a straight line was reasonably good. These calibration curves were prepared with only one exposure for each concentration, whereas calibration curves compiled for the literature by DC arc techniques were the averages of 8 to 16 exposures for each concentration.

These calibration curves and sensitivity data for oxygen as a function of argon concentration indicate that any concentration in this range will be satisfactory.

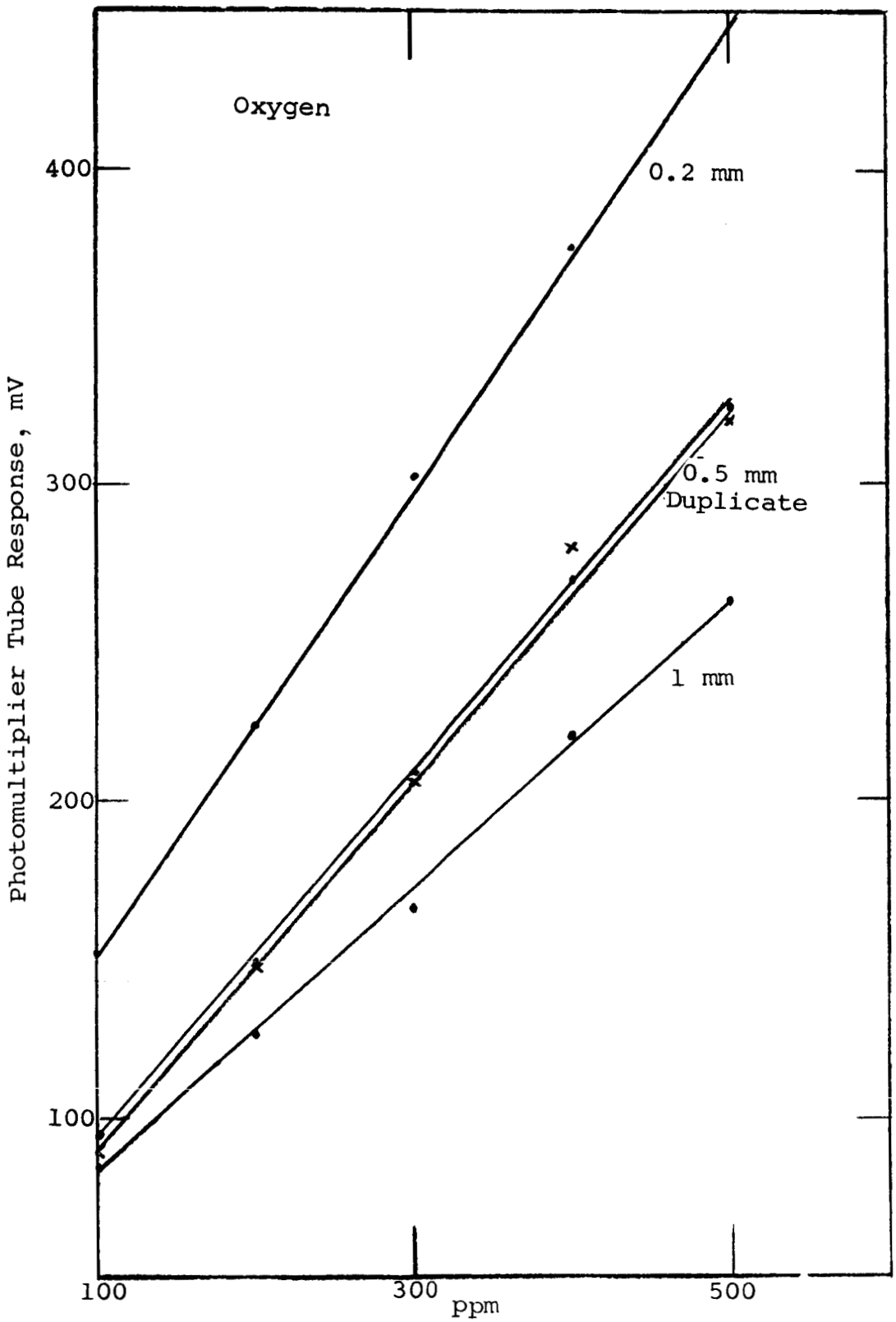

Figure 13

EFFECT OF ELECTRODE IMAGE DISTANCE FROM APERTURE ON RESPONSE OF PHOTOMULTIPLIER

Initial calibration curves for concentrations less than 100 ppm prepared on alloy 2024 were quite poor. In the preparation of plate 1345 (Figure 14), the work metal was prewarmed with two to three passes, 80 sec per pass. A low flow of shield gas was maintained between each weld pass. Each point represents exposures from fresh, properly cleaned surfaces.

The same care was used in securing the data for plate 1346 (Figures 14 and 15), except that a weld pass with clean shield gas was made over the new surface and then the desired quantity of contaminant was added for the next pass. The heterogeneous location of points seems to indicate that a nonhomogeneous concentration of contaminants at the surface of the alloy was reduced or more evenly distributed by the pass and apparently reduced to a constant level. The change in the slope at the lower end of the calibration curves indicates the presence of residual contaminants either in the metal or in the shield gas.

The spectral response resulting from adsorbed surface contamination is shown in Figure 16. The concentration of the hydrogen being added was a constant 80 ppm. The first reading was taken about 2 min after striking the arc on a cold plate. The high initial readings are believed to be due to adsorbed moisture, since the change was minor after the work metal became quite warm and showed a steady decline as the work metal became hot and the moisture was desorbed.

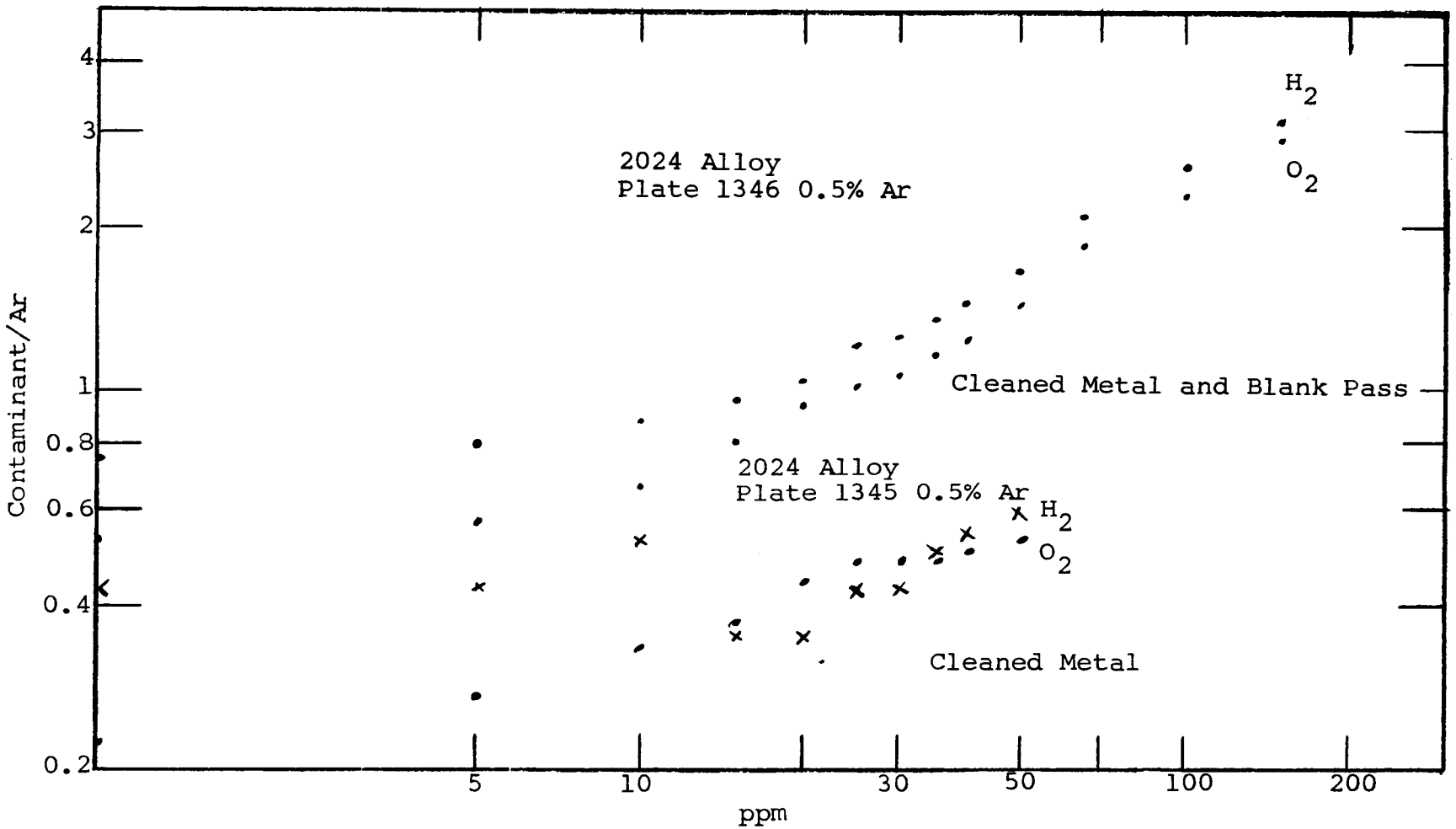

Figure 14

EFFECT OF SURFACE METAL CONDITION ON SPECTRA OF PLATES 1345 AND 1346

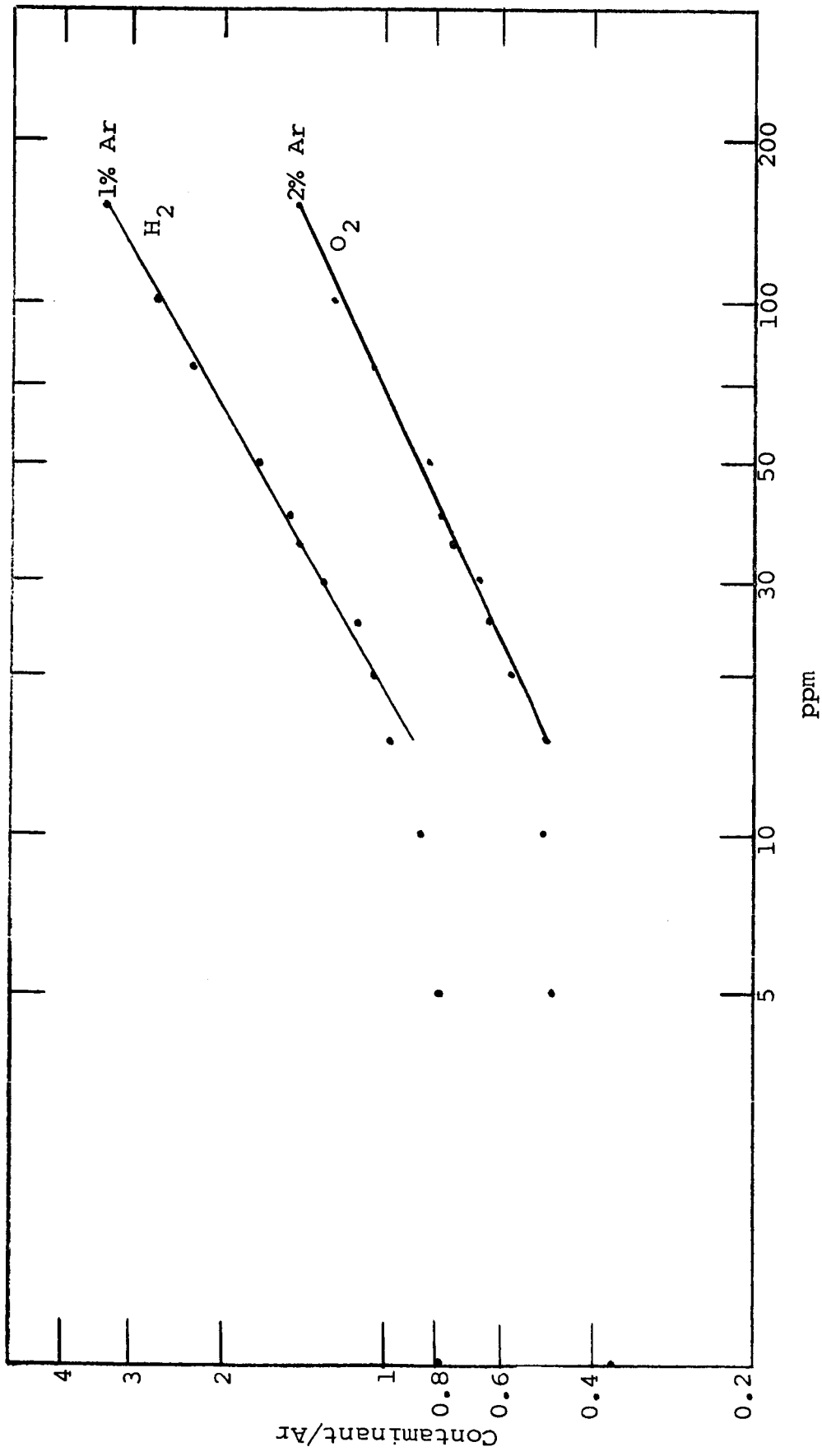

Figure 15

DEVIATION OF POINTS WITH GREATER ARGON FLOW RATE WITH BLANK PASSES

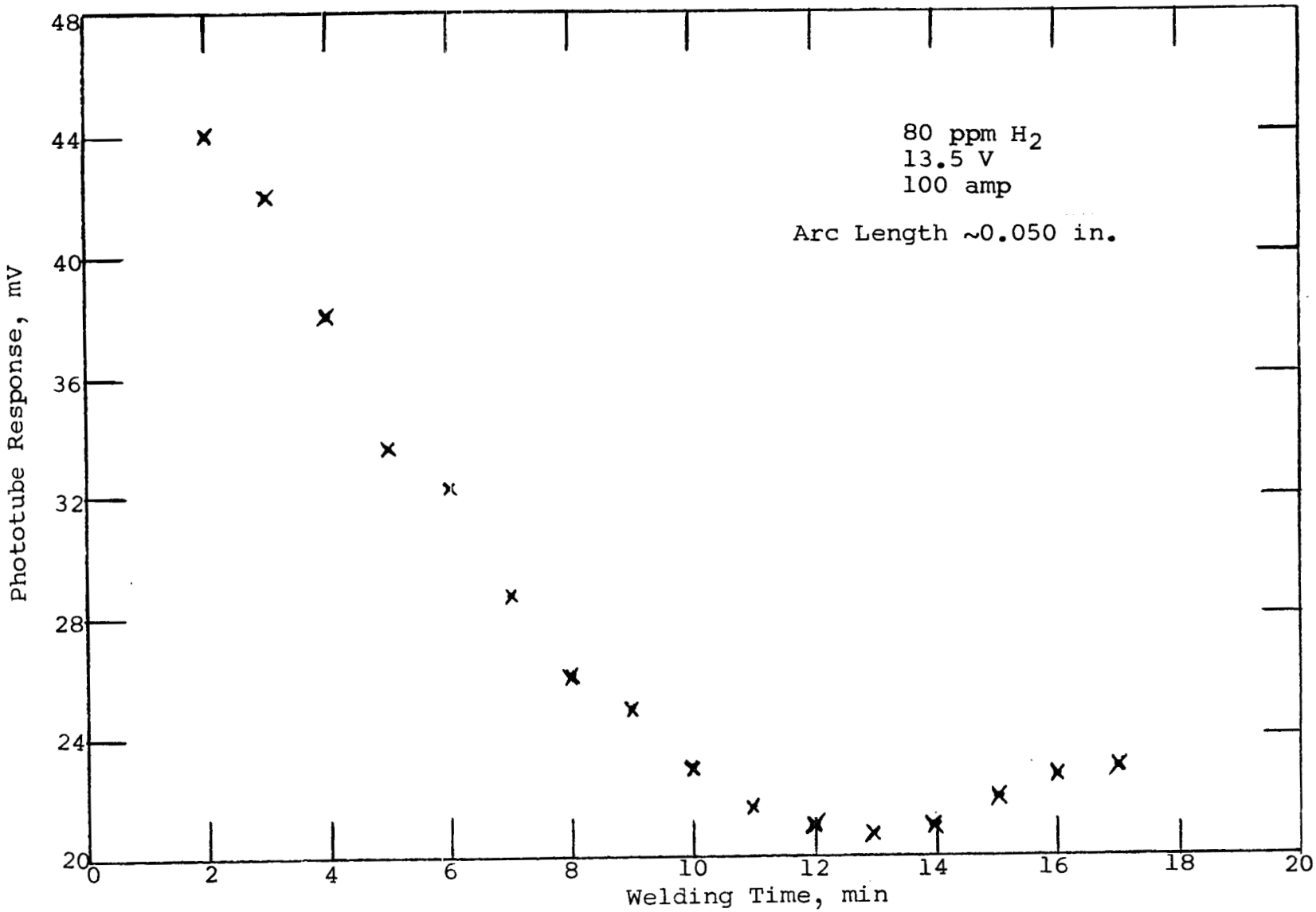

Figure 16

EFFECT OF TIME AFTER COLD START ON RESPONSE OF PHOTOMULTIPLIER

Calculated ratios based on the readings of photomultiplier tube response for hydrogen with 2% argon (Figures 17 and 18) were prepared by using the fiber optic bundle with the optical system. This optical system was not very efficient. Hence the output readings were low and varied considerably. Thus there is a noticeable lack of linearity of individual points. However, Figure 18 shows the much better reproducibility of calculated ratios from conditions that produced two entirely different directly measured curves for hydrogen.

With slightly longer arc lengths both the directly measured curve (Figure 13) and the calculated ratios (Figure 19) show greater precision with respect to linearity and reproducibility.

A temporary optical device was prepared to greatly magnify the electrode gap and image this on a screen. Although the welding machine was supposedly operating at a constant gap length, the variation during a pass and from pass to pass was considerable, even though no settings had been changed.

Results obtained when tracings from the direct ratio readout system, the Devar multiplier-divider module, was used are shown in Figure 20.

6. Arc Length and Voltage Drop

The spectroscopist normally thinks in terms of arc length, while the welding engineer records the voltage. We briefly explored this point since voltage can vary according to the

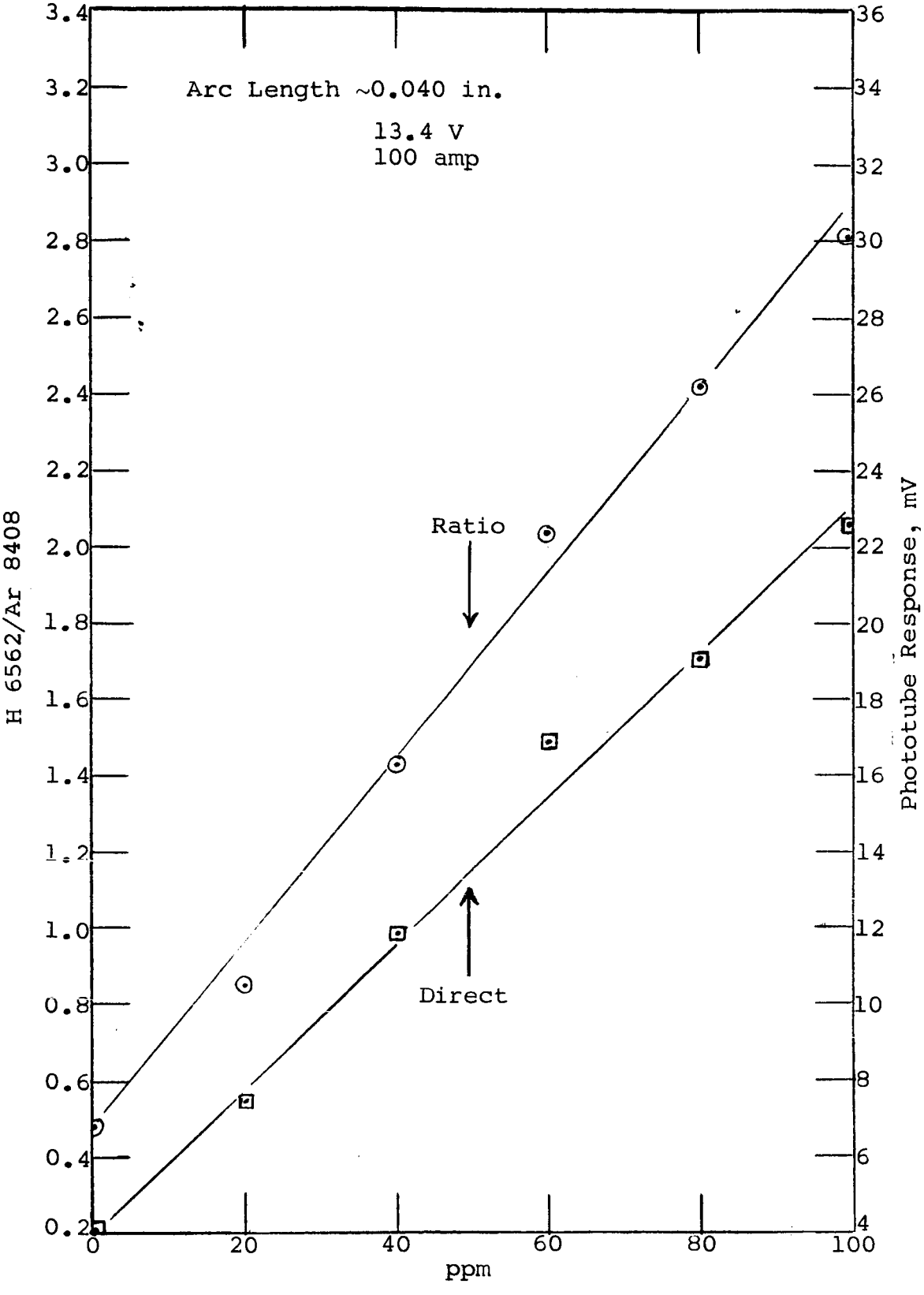

Figure 17

CALIBRATION CURVE FOR HYDROGEN

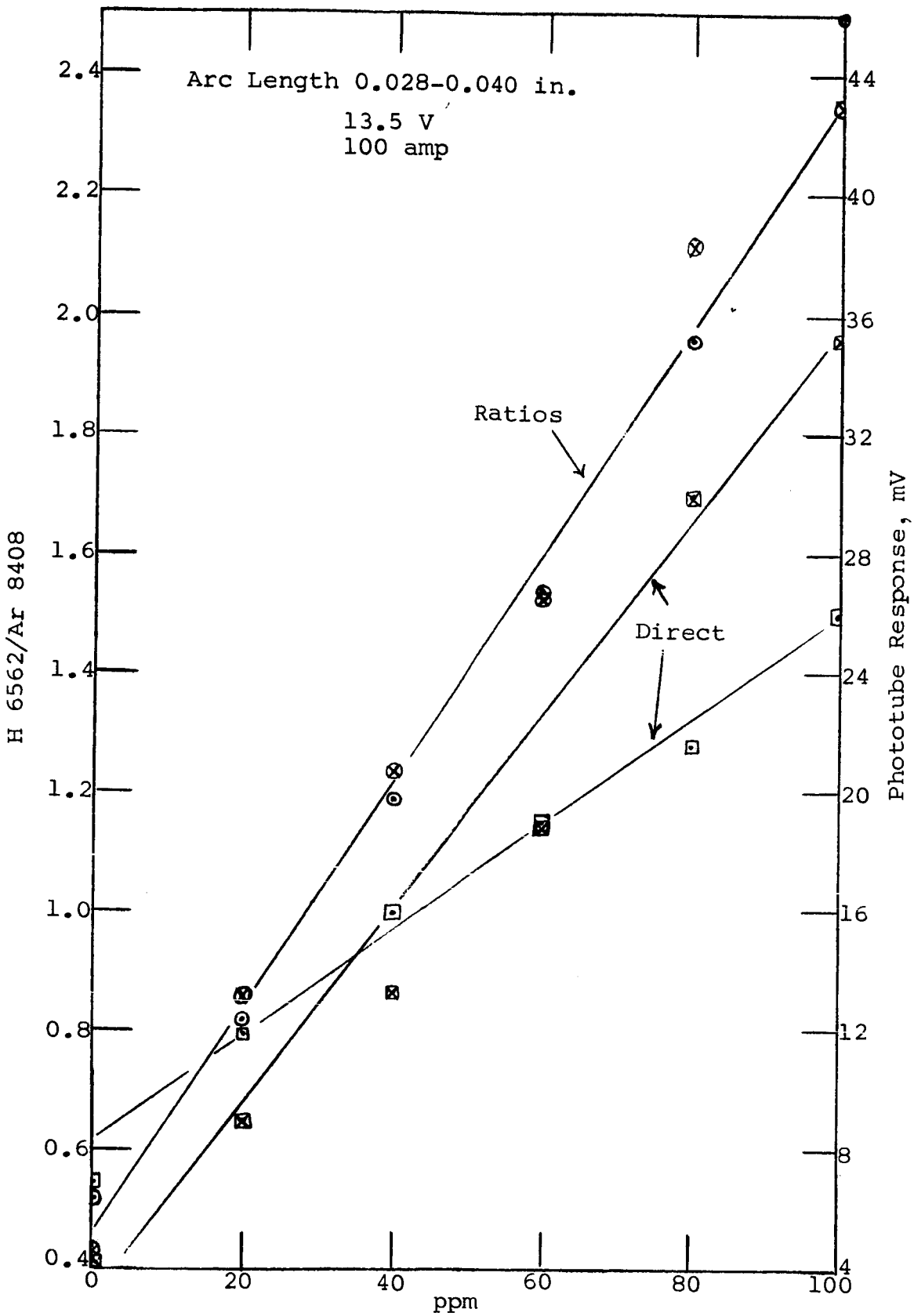

Figure 18

RESULT OF DUPLICATE RUNS

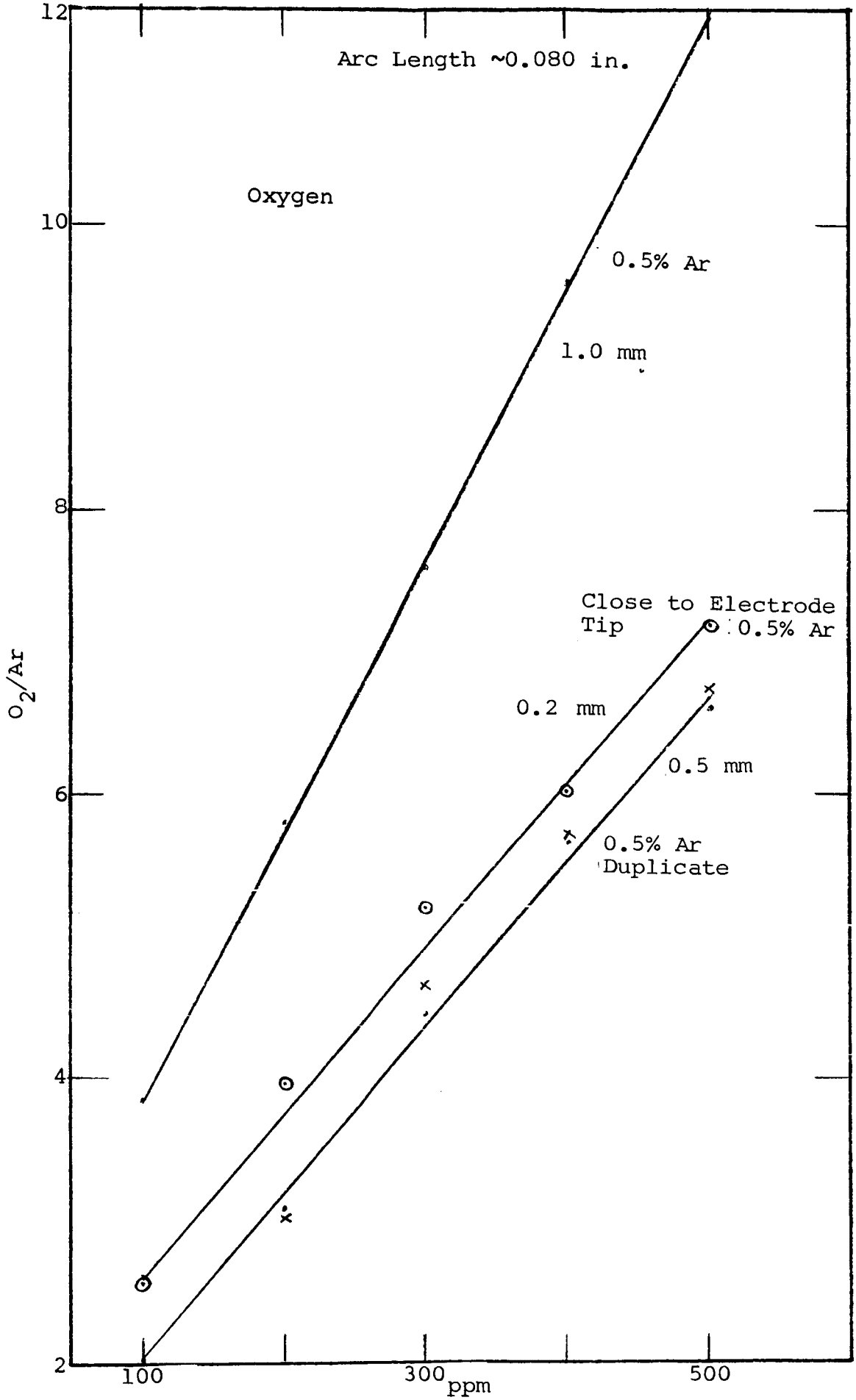

Figure 19

CALCULATED RATIOS

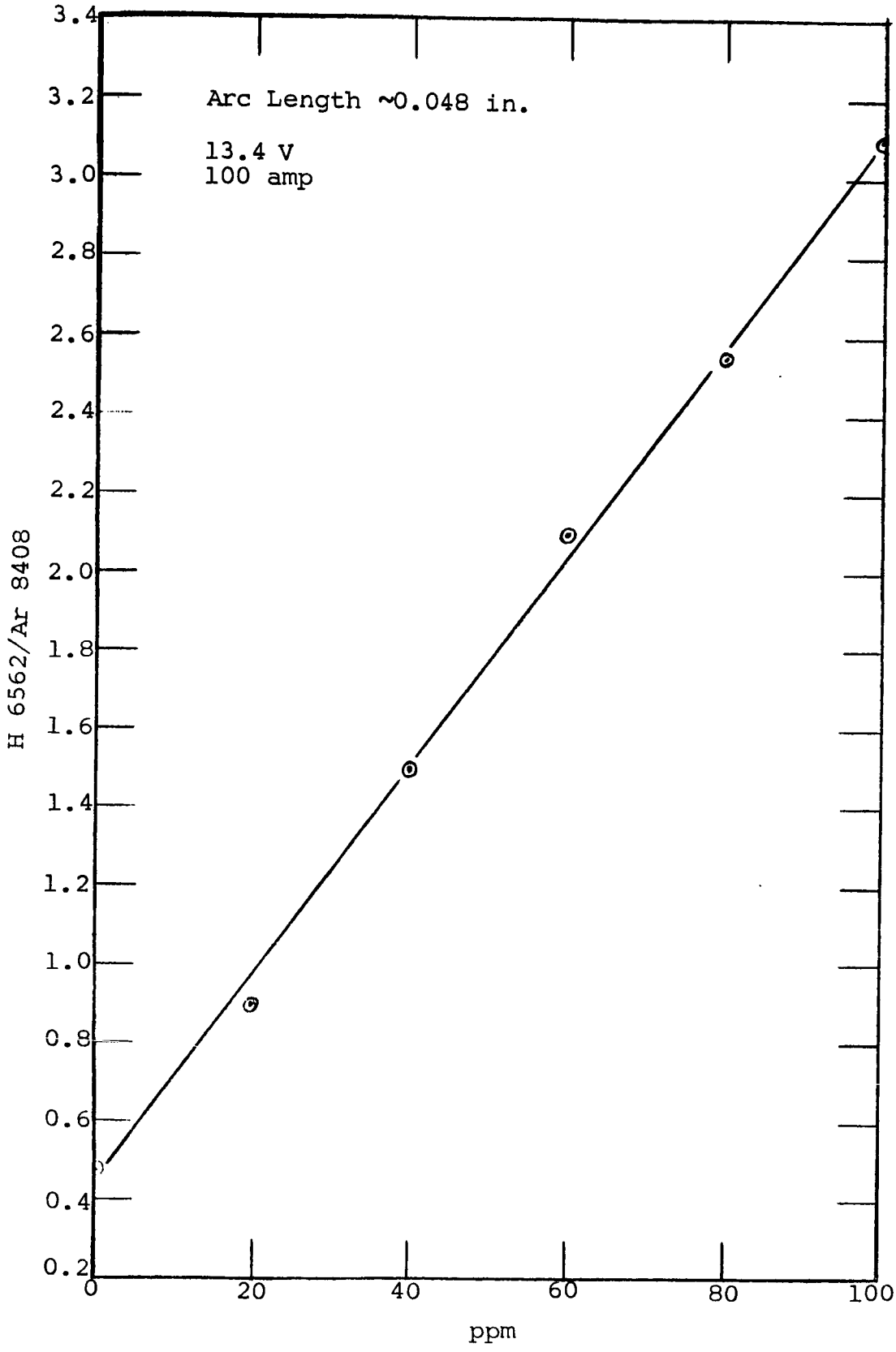

Figure 20

DIRECT RATIO READOUT

machine and the position of the connecting leads. We were unable to develop any correlation between our voltage readings and arc-gap measurements, nor could we correlate the data sent us by NASA, Huntsville.

7. Blackbody Radiation and the Optical Wedge

A spectroscopist allows his instrument to view only a portion of the arc between two electrodes of some constant convenient length, such as 2 to 3 mm (1 mm = 0.040 in.). Blackbody radiation is masked by the diaphragm of the limiting aperture. In addition, the optical axis is vertical to the axis of the electrodes.

For aluminum welding, in which very short arcs are required, the adjusting of the electrodes to mask the blackbody on the aperture diaphragm is very critical. The size of the work metal is such that the optical axis cannot be at a right angle to the electrode; thus the degree of blackbody radiation may be zero for one current and carriage speed, but not for a second. Varying either factor could increase the size of the molten puddle so that the blackbody may increase sharply. Another factor observed was the reflection of the arc on the smooth plate surface. At given close distances part of this reflection was viewed by the limiting aperture, which behaved in a manner similar to but less intense than the blackbody radiation from the electrode. There were large changes in the photomultiplier output whenever the optical system was adjusted to view this reflection.

The internal standard technique will not compensate for gross changes such as these, partly because the dispersed background level is different at the different wavelengths.

The principle of the optical wedge was studied to overcome this problem. If an optical wedge (Figure 21) is caused to oscillate in front of a light beam from an entrance slit, the changing thickness of the wedge produces a change in the amount of the refraction of the light beam. This causes the spectral line to oscillate across the exit slit (Figure 21). The thermal background can be a varying DC signal, but the oscillation of the line intensity results in a pulsing DC, effectively an AC, output that is separated from the thermal background.

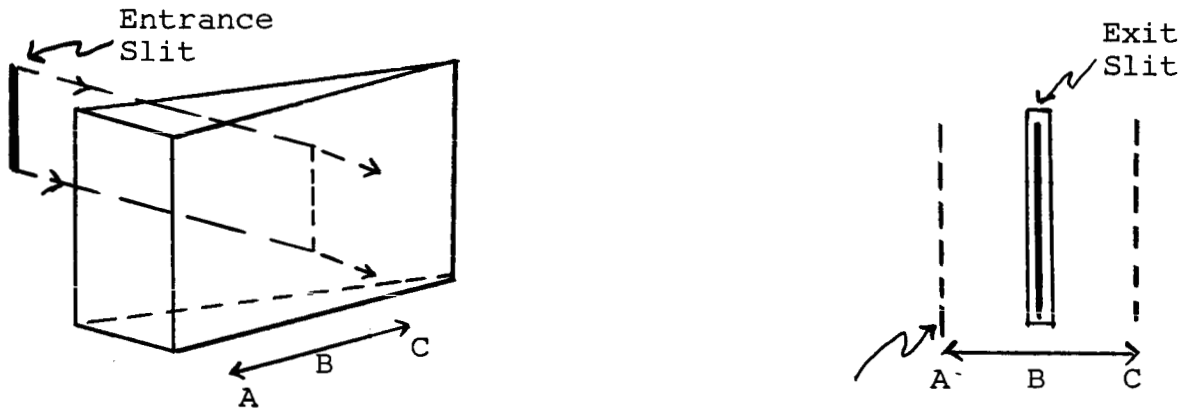

Figure 21

OSCILLATING WEDGE AND OSCILLATION OF SPECTRAL LINE

A simple wedge device subject to little wear is a circular optical wedge mounted on a 300-rpm synchronous motor such that the light beam passes through one side (Figure 22). The spectral line does not follow a true horizontal oscillation but has a slightly circular pattern. However, this causes no trouble and is presently being used. For electronic readout, an oscilloscope (AC input) and a Ballantine model 300 electronic AC voltmeter were both connected across the photomultiplier tube load. The deviation of the wedge was adjusted to give a sinusoidal-like 10-cps output, indicating a symmetrical sweep on both sides of the line.

The influence of the wedge was demonstrated with a constant amount of hydrogen by varying the length of the arc and also by introducing the glow of the hot electrode into the aperture. No difference in the wave height on the oscilloscope was noted.

This concept solved the problems associated with background, reflections, and arc length. Time did not permit more evaluation, since construction of the spectrometer required all the available time.

8. Noncatalogued Emission Lines

Difficulty was experienced in studying the photomultiplier tube response for the nitrogen 8216 A line. When the nitrogen concentration was changed or when it was reduced to zero, there was no change. When the spectrum was scanned for

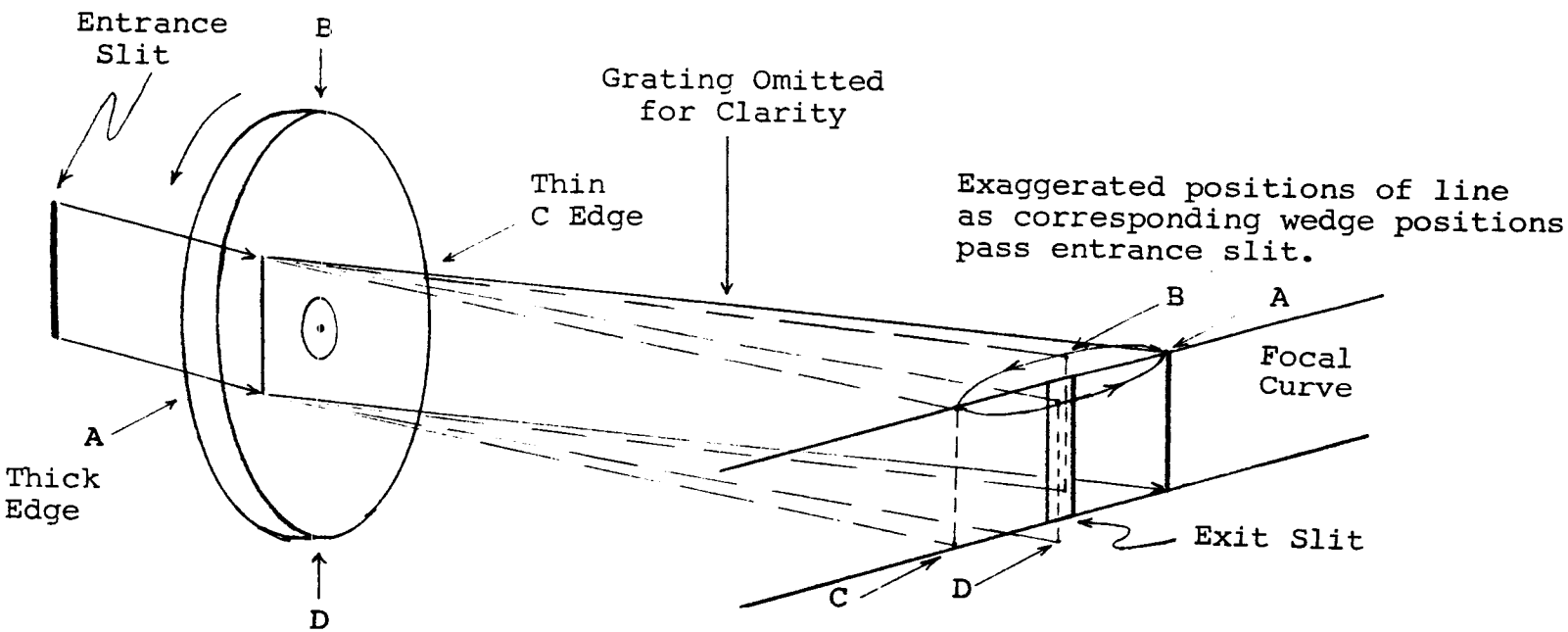

Figure 22

ROTATING CIRCULAR WEDGE AND LINE MOTION ON FOCAL CURVE

other specific lines, strong photomultiplier tube responses were occasionally observed at unexpected wavelengths. According to photographed spectra for pure aluminum, emission lines should not be present at these wavelengths. Aluminum alloy 2024 was used as the work metal at this time.

Several spectra were photographed at different current densities and arc lengths. Several unknown well-defined lines as well as several rather broad diffuse lines were found. The wavelengths were calculated, but none could be identified through the available tables and atlases. Numerous tests were performed to ensure that these lines were excitation lines and not reflections.

One line was so close to the 8216 A nitrogen line that the exit slit on the 3.4-meter spectrograph did not exclude it. Thus it would not be possible to exclude it from the nitrogen 8216 A line with the small spectrometer. A second broad and diffuse line, approximately 6544 A, was found near the hydrogen 6562 A line, but it was far enough away that it probably could be masked.

Thirteen unknown lines, very strong to moderately strong, were found in this region. Most were identified as magnesium III lines. The lines were not identified from the literature but from the low-current arcing of very pure metals in a helium atmosphere.

Because of the spectral interference by the unknown line for the nitrogen 8216 A line and because the preliminary porosity study indicated that nitrogen in helium had no deleterious effect on the weld bead, nitrogen was dropped from the elements to be monitored.

Later the spectra were photographed by using aluminum alloy 2219. None of these lines appeared, and the background decreased to a much lower level. Thus this also indicated that these new lines and the high background were largely due to the magnesium in the 2024 alloy.

B. Electronic Design Criteria

1. Choice of Photoelectric Sensor

In order to sense the energy of emission lines at the required wavelengths, the sensor must have the following general characteristics:

(1) Fairly large sensitive area

(2) Spectral sensitivity from the mid-visible to the near-infrared region

(3) Linearity over a wide range of light inputs

(4) Sensitivity essentially independent of ambient temperature

(5) High sensitivity to light input.

The combination of these properties appears to rule out the available semiconductor sensors and to favor the photoemission (phototube) sensor. The performance of the simple vacuum phototube satisfies all these requirements except the last. The multiplier phototube (photomultiplier) has the required high sensitivity in addition to the other properties. The data in the following paragraphs indicate why the photomultiplier is necessary and why this type of photomultiplier tube was chosen.

2. Required Spectral Response of Photoemission Sensor

The major spectral emission lines studied for the monitoring instrument included:

Hydrogen	6562.9 A
Oxygen	7771.9 A
Nitrogen	8216.5 A
Argon	8408.2 A 8521.4 A 7147.5 A

In order to detect the spectral range from 6500 to 8550 A, the S-1 phosphor is required. This phosphor has two peaks, one in the near-ultraviolet at 3500 A and one in the near-infrared at 8000 A. The latter peak is quite broad, and a near maximum response is obtained through the above range of spectra. The S-20 phosphor approaches the required range, but its response falls off rapidly at wavelengths longer than 8000 A.

3. Phototube versus Photomultiplier Tube

Initial experiments were conducted to compare the RCA type 917 vacuum phototube with the RCA type 7102 photomultiplier. Both tubes utilize the S-1 phosphor. The 917 is a sensitive phototube with a reasonably large cathode area. The 7102 is one of the few photomultipliers with the S-1 phosphor that is readily available; it is an end-cathode tube and has a comparatively low dark current. The Dumont type 8062 has similar characteristics, including base dimensions, but has a somewhat smaller cathode area.

A suitable mounting and bridge circuit was constructed for the 917 phototube. An Eldorado microphotometer was fitted with a 7102 photomultiplier, and tests were run on the oxygen emission line at the 500-ppm level of oxygen in the inert shield gas. No response was observed with the phototube. The photomultiplier gave an output of 1.0 μamp at an operating sensitivity of 5 μamp per microlumen. The phototube response (if it could have been observed) would have been only 1/100 of its dark current and thus was well beneath its noise level. The RCA 7102 was thus chosen as the operating detector for the contamination lines of interest.

4. Criteria for Internal Standard and Light Chopping

For direct-reading spectrometers with an internal standard the signals are normally integrated as a function of time. In this method, the energy sensed for the internal

standard is integrated (as in the charging of a capacitor) until a certain predetermined energy level is reached. At this point the signal from the analytical lines of interest are at a related level and are automatically read out; the procedure is then repeated. In the present application, where an immediate response time was desired, an on-line type of readout is effectively needed. This was accomplished by the use of a ratio computer in each analytical and internal standard photomultiplier circuit.

Exploratory work was necessary to evaluate the type of internal standard. The nondispersed light from a beam splitter to be used as the internal standard was sensed by a type 917 phototube and a DC readout circuit. At the same time a given analytical line was monitored by using a type 7102 photomultiplier. For this experiment, as well as for succeeding ones, a special photomultiplier bridge and balancing circuit feeding into a DC electronic microvoltmeter were used in place of the Eldorado in order to obtain adequate dark current balancing capability. The resulting average signal levels obtained with various types of arcs are given in Table 1.

Note from Table 1 that even though the phototube values are in the microvolt level, they can be read with this type of instrument. However, from multichannel recordings the nondispersed channel did not vary in the same manner with the emission line channel under various conditions. Thus the

Table 1

OUTPUT SIGNAL FOR THE DIFFERENT ARC SOURCES

Contaminant, ppm	Type of Arc or Weld	Arc Current, amp	Photomultiplier Signal, V	Photomultiplier Background, V	Phototube Signal, μV
100 O_2	Arc stand	15	0.25	0.08-0.13	80-220
300 O_2	Arc stand	15	1.1	-	-
200 O_2	Drum	100	1.3	0.3	550
500 O_2	Drum	100	2.5-3.0	0.3	550
200 H_2	Drum	100	1.0-1.3	0.18-0.4	600-800
500 H_2	Drum	100	3.5-4.0	-	500-800
500 N_2	Drum	100	0.6	0.1-0.4	300
50 O_2	Plate	250	0.55	0.08-0.10	250
100 O_2	Plate	250	0.62	0.08	210
300 O_2	Plate	250	1.3	-	180
500 O_2	Plate	250	1.9-2.0	-	-

nondispersed phototube type of internal standard was not suitable. Table 2 shows additional signal levels obtained with 1-in. aluminum plate welding; these data include various argon lines that can be used for the internal standard. (A small quantity of argon was added to the helium shield gas.) The 3.4-meter spectrograph was used for these experiments.

As shown in Tables 1 and 2, whereas the photomultiplier signal readings are in the volts range, the photomultiplier background readings are a sizable portion of the total readings. (In Table 2 the background reading is the 0 ppm reading.) These tables do not include the dark current values, which also were a sizable portion of the total (ranging from 0.4 to 0.8 V). One-megohm photomultiplier and phototube load resistors were used throughout, equating microamperes to volts.

An on-off light chopper with an AC amplification system is generally used to solve the dark current problem, but this does not solve the background level (arc background) problem. The latter was solved by using an optical wedge, which acts as a chopper. This type of chopper shifts the spectrum line back and forth across the exit slit during each revolution. Thus the peak-to-peak AC signal that results is proportional only to the difference in energy between the emission line and the total background. This technique was tried experimentally by using a Ballantine model 300 AC vacuum tube voltmeter capacitively coupled to the photomultiplier anode. The wedge disc

Table 2

SIGNAL AND BACKGROUND VOLTAGES FOR THE 1-IN. PLATE WELDING

Line, A	% Argon to Helium Shield	Contaminant, ppm	Arc Current, amp (avg.)	Photomultiplier Emission Line, mV	Phototube (Nondispersed), μV (avg.)	Entrance Slit, μ
6965 Ar	0	none	160	20	120	50
	0.5	none	160	60-70	120	50
7384 Ar	0	none	160	13-14	100	50
	0.5	none	160	75-90	100	50
8408 Ar	0	none	160	7-9	120	50
	0.5	none	160	120-150	120	50
7771 O_2	0	none	175	27		50
	0	100 O_2	175	70		50
	0	200 O_2	175	110		50
	0	300 O_2	175	130		50
6562 H_2	0	none	180	100	80	50
	0	100 H_2	180	225	80	50
	0	300 H_2	180	350	80	50
	0	500 H_2	180	500	80	50
7771 O_2	0	none	180	350	500-600	700
	0	100 O_2	180	550	500-600	700
	0	300 O_2	180	1,300	500-600	700
	0	500 O_2	180	1,800	500-600	700
6562 H_2	0	none	180	1,200	400-420	700
	0	100 H_2	180	2,400	400-420	700
	0	300 H_2	180	5,000-5,500	400-420	700
	0	500 H_2	180	7,500-7,700	400-420	700

was rotated at 5 rps, giving a 10-cps signal (two peaks were obtained for each revolution). This concept solved the dark current problem and also the high-level background problem from blackbody radiation.

III. DESIGN AND CONSTRUCTION

A. Optical System

1. Basic Design Requirements

A basic optical design with the least number of optical parts for alignment was considered best for this spectrometer. The design is essentially a fixed Eagle mount and a modification of the Rowland circle principle, which consists essentially of three parts: the slit, the concave grating, and the camera (in this case photomultiplier tubes). The concave grating acts both as the dispersing and focusing device, and no collimating lens or mirror is necessary. The slit, grating, and camera (photomultiplier tubes) are fixed on the Rowland circle, and the spectrum of interest is in focus at all times.

The spectral region was determined by using the available analytical lines for hydrogen and oxygen. The 6562.8 A hydrogen line is the only sensitive line for this element in the near-ultraviolet and visible spectrum. The 7771.9 A line is the only oxygen line close to the hydrogen line. In this region the strongest nitrogen line, although it is still relatively weak, is the one at 8216.4 A.

The S-1 response tube, available only in the end-on type of photomultiplier, is needed for this spectral region. These tubes, including the shield and bracket, are 1.88 in. in diameter, and with the socket approximately 5 in. long. If these tubes are to be mounted on the focal curve to monitor the oxygen 7771.9 A and the nitrogen 8216.4 A lines, the very minimum reciprocal dispersion possible is 15 A/mm. If this dispersion were used, however, the tubes would be off-center. A value of 14.6 or 14.1 A/mm would be better, although this is a high reciprocal dispersion for a small instrument. A very long focal curve with respect to the radius of curvature is required to cover the spectral region.

After the grating specifications had been established, nitrogen was deleted from the required elements because of its observed spectral interference with the 8216 A nitrogen line when 2024 aluminum alloy was used and because nitrogen appeared to have no deleterious effect on weld bead quality.

2. Grating and Optical Design

In order to meet system requirements, a grating was designed. The concave grating has an 82- by 56-mm grooved surface, a 60-cm radius of curvature, and 610 grooves/mm (approximately 15,000 grooves/in.). The grating was blazed in the second order for the 6400- to 8400-A region. This instrument has a speed of approximately f/8.

To establish the required parameters of the grating, several calculations were required.

$$m\lambda = \frac{A}{N} (\sin i \pm \sin Q) \qquad (1)$$

where

m = order

A = linear aperture of the grating

N = total number of grooves

i = angle of incidence of light on the grating

Q = angle of diffraction.

By differentiating the grating equation (Equation 1) with respect to wavelength, λ (i is a constant with respect to λ), the angular dispersion equation is obtained:

$$\frac{dQ}{d\lambda} = \frac{N\ m}{A\ \cos\ Q} \qquad (2)$$

By combining Equation 2 with that for linear dispersion (Equation 3) and taking its reciprocal, the formula for plate factor for the grating is obtained (Equation 4).

$$\frac{dl}{d\lambda} = r\ \frac{dQ}{d\lambda} \qquad (3)$$

$$\frac{d\lambda}{dl} = \frac{A\ \cos\ Q}{N\ m\ f} \qquad (4)$$

where

f = radius of curvature.

For an approximation, assume cos Q = 1; then the reciprocal dispersion is approximately 14.1 A/mm. This establishes the grooves per inch required to produce the space needed between

photomultiplier tubes on the focal curve. However, since $\angle Q$ is not 0, the reciprocal dispersion will be less and will vary as a function of wavelength.

Very close reciprocal dispersion tolerances could not be obtained by varying the number of grooves per inch by a small quantity such as 1000 or 2000 grooves. Gratings are ruled in multiples such as 7500, 15,000, or 30,000 grooves per inch because of the settings and controls on modern ruling engines.

The angle of incidence normal with the grating was found to be 19° (Figure 23), which places the hydrogen 6562 A line as close to the entrance slit as possible. If the optimum angle of 23° were used, the hydrogen line would be refracted back very close to the entrance slit. For this reason the angle of incidence would also influence the reciprocal dispersion.

By calculating Q in the grating formula (Equation 1), the following angles were obtained.

Hydrogen	6562.8 A	28°22'	cos Q = 0.8799
Oxygen	7771.9 A	38°30'	cos Q = 0.7826
Argon	8521.0 A	45°34'	cos Q = 0.7001

Therefore the reciprocal dispersion becomes:

6562.8 A	12.4 A/mm
7771.9 A	11.0 A/mm
8521.0 A	9.9 A/mm

Then the distance, r, from the center of the grating to the point of focus on the focal curve can be calculated from

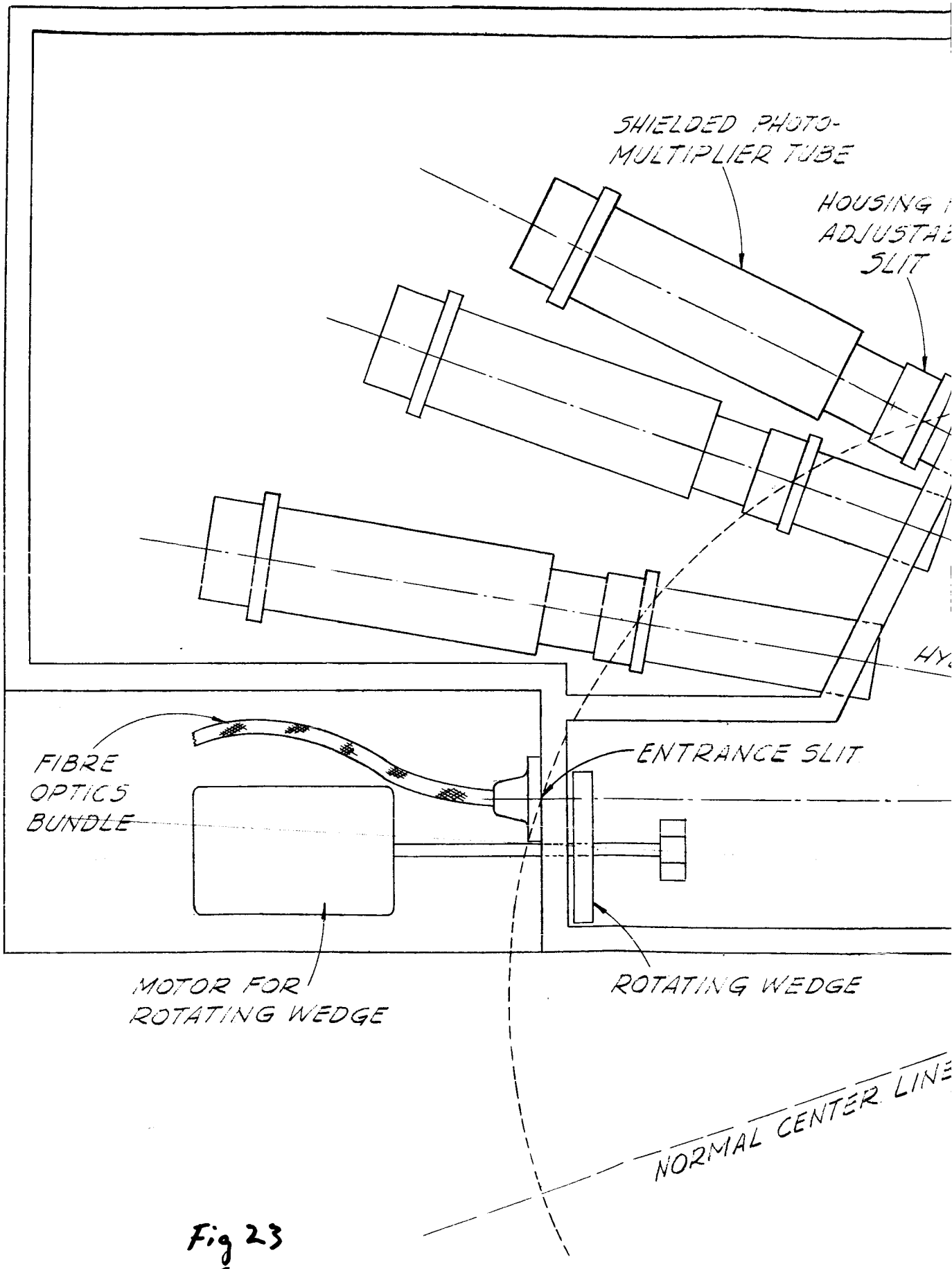

Fig 23

Figur

OPTICAL

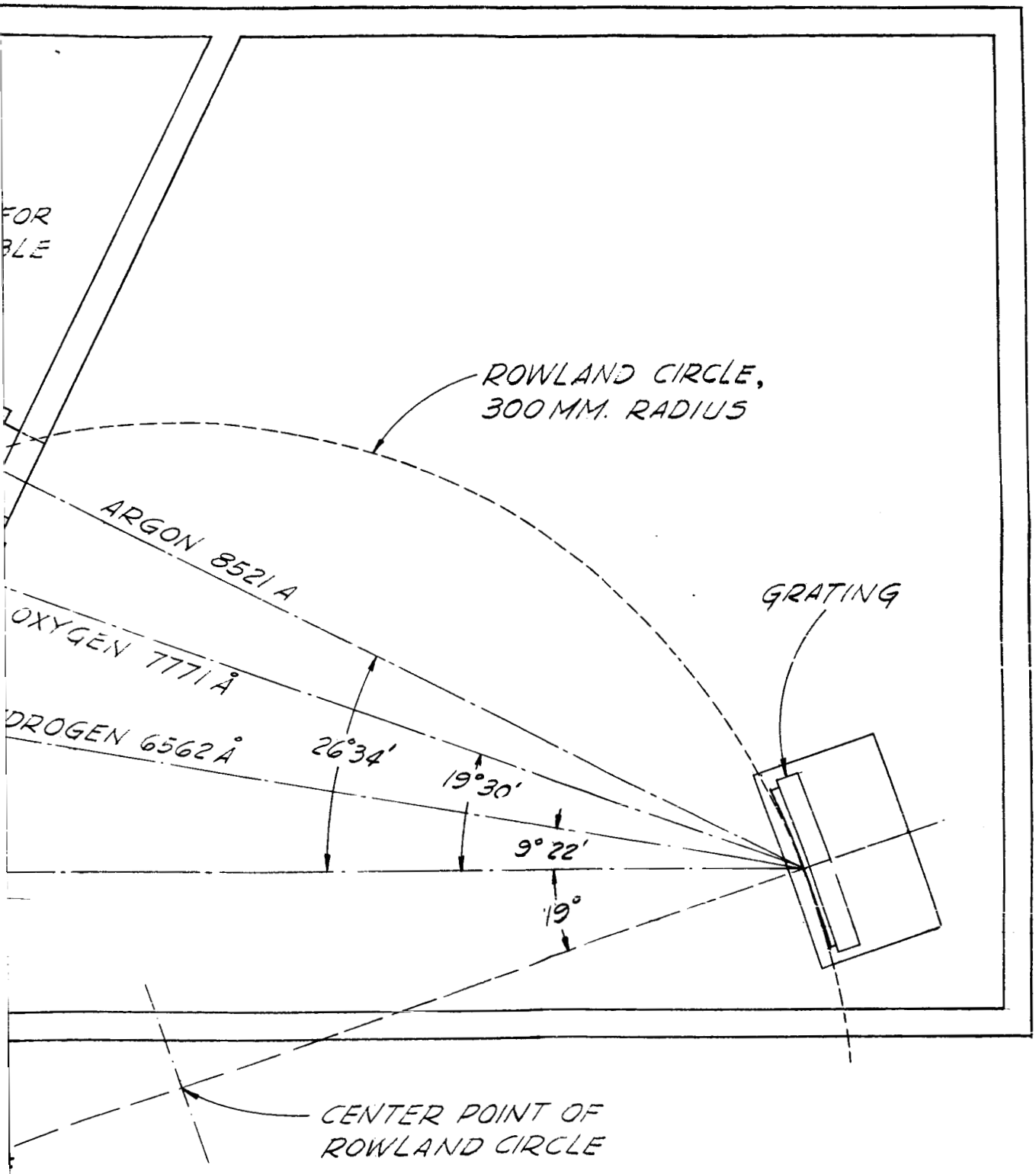
FOR
BLE
ROWLAND CIRCLE,
300 MM. RADIUS
ARGON 8521 A
OXYGEN 7771 Å
DROGEN 6562 Å
26°34'
19°30'
9°22'
19°
GRATING
CENTER POINT OF
ROWLAND CIRCLE

Fig 23 (2)

the equation for linear dispersion (Equation 3). The exit slits for the photomultiplier tubes are located at these positions:

6562.8 A	530.1 mm
7771.9 A	473.2 mm
8521.0 A	430.2 mm

The overall layout is drawn according to scale in Figure 23. Nitrogen at 8216 A was not included since this gas did not influence the aluminum welding. The 8521 A argon line was used as the internal standard in place of the previously planned 8408 A line. The 8428 A argon line is so close that it limits the sweep from the optical wedge and a proper wave form signal is not possible.

The optical compartment is actually divided into two parts separated by a solid light-tight barrier. One part contains the entrance slit, grating and mount, and the optical wedge; the other part contains the exit slits, photomultiplier tubes, and mounts. The exit slit for each emission line was located on the focal curve in the calculated position, and the positions were checked experimentally. Slit-extension tubes, 1-3/8 in. ID, extend from the exit slit assembly through the barrier wall.

With this two-compartment arrangement it is possible to adjust the exit slits with the instrument in operation. Photomultiplier tubes can also be replaced without disturbing

the optical alignment. The barrier wall also adds strength and rigidity to the case.

The case was made from Bevelax 100A, a material recommended by the Mechanical Engineering Division. This material is highly resistant to moisture and thermal effects. All joints except those for the lids were joined with epoxy resin and bolts.

3. Grating and Mount

The grating block is borosilicate glass, 56 by 82 by 12 mm. The dimensions of the face are 50 and 76 mm. An offset edge, 3 by 3 mm, was ground on each of the four sides of the blank so that it could be held behind a frame with the concave face projecting in front of the mount. Thus the grating is mounted in a specially designed shock-resistant mount, so that the grating cannot become dislodged and damaged. The basic details of the grating and mount are shown in Figure 24.

Between the frame and the offset edge, the tolerance is only 0.005 in., and between the grating blank and the walls of the mount, 0.010 in. Thus the frame also acts as the centering device. The grating is held against the front retaining frame by three flat 0.020-in. phosphor bronze springs. This provides equivalent pressure at all points so that there will be no distortion due to pressure, which would be the situation if the frame held the grating blank against the back wall of the mount.

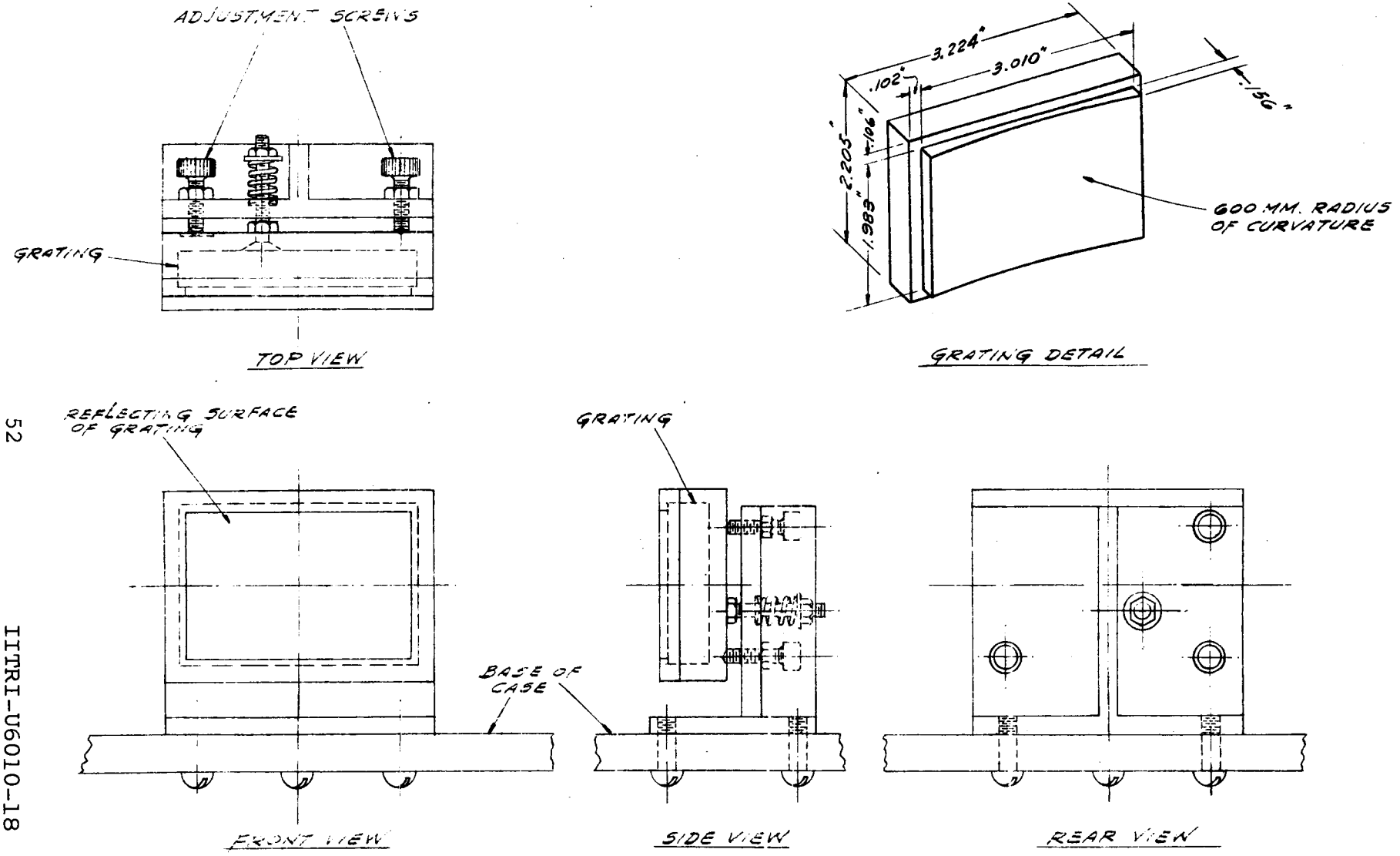

Figure 24

ASSEMBLY OF GRATING

4. Optical Wedge-Slit System

The optical wedge is a circular glass disc ground 3.3° off parallel; it is driven at 300 rpm with a Borg synchronous motor (Figure 23). The disc is placed 1 in. from the entrance slit. In this position the emission lines sweep through a distance of 3.5 mm at the exit slit. The grating is basically filled at all times during a rotation.

The entrance slit is the end of the fiber optic bundle and is 1 mm wide and 19.8 mm high. This 1-mm slit, which is considered very wide, is used to bring in as much light energy as possible and compensates for the light loss due to the fiber optic bundle. This wide slit is possible since high resolution is not necessary and since no close lines from the argon-helium shield gas and 2219 aluminum alloy are present to interfere with the analytical and internal standard lines.

The face plate for the entrance slit should be at a right angle to the incident ray of the grating. However, because of the diffraction due to the optical wedge, the face plate is set at 91° to compensate for the effect of the wedge.

The exit slits are 2 mm wide and 22 mm high. The 22-mm-long exit slit permits the total image of the entrance slit to be viewed by the photomultiplier tube, since there is a small vertical oscillation due to the optical wedge.

The exit slit arrangement and photomultiplier tube housing assembly are shown in Figure 25. The overall length of the tube shield, which includes the space for socket connections,

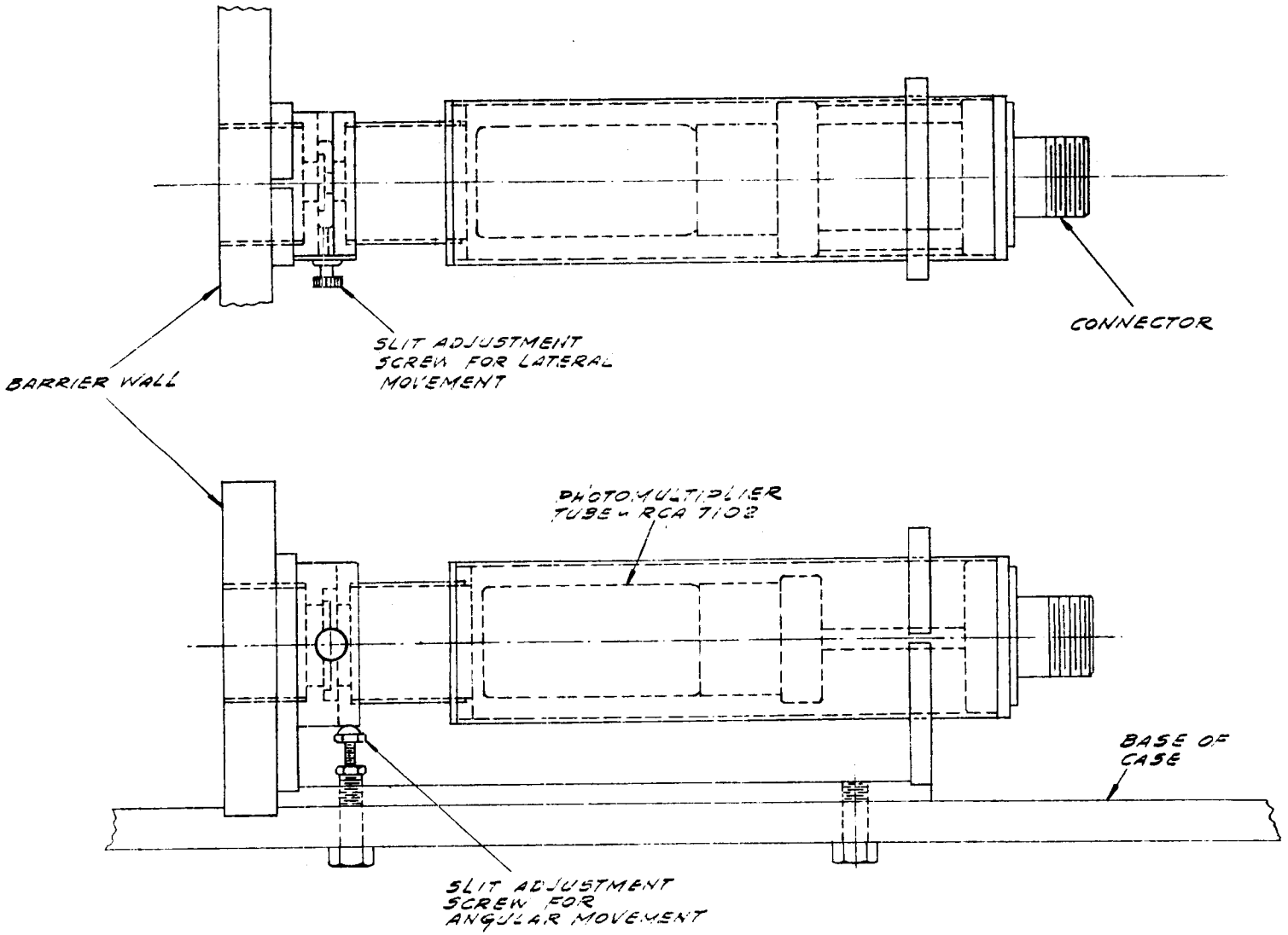

Figure 25

ASSEMBLY OF PHOTOMULTIPLIER TIBE

is 6-3/4 in. The connector tube between the slit assembly and the photomultiplier tube housing is 1-13/32 in. This space permits the emission line to defocus and cover a greater area of the cathode. The base plate for this assembly is 8 in. long. The center of the assembly is 2.062 in. above the base of the case. The overall length of this assembly could have been reduced by the use of shorter tube-to-socket beads and smaller AN connectors. This in turn would have permitted the use of a smaller overall case (Figure 23).

The exit slit can be adjusted in the lateral direction with a screw adjustment. The vertical adjustment is also accomplished by means of a screw locknut arrangement at each corner of the slit assembly. These screws fit in the base plate bolts that were drilled and tapped for this purpose. The jaws of the exit slits are prepared from 1/64-in. razor blade steel and mounted with small screws. The sharpened wedges serve as the exit slit jaws.

Brass was used in constructing these parts as well as those for the grating mount.

5. Fiber Optic Bundle

The fiber optic bundle was prepared such that the entrance slit and limiting aperture ends had the same dimensions, namely, 1 by 19.8 mm. The fibers are 0.004 in. in diameter and are parallel so that the bundle is very nearly coherent. The core material is Shott F-2, N_d = 1.62, glass rod, and the coating is Kinble R-6 glass, N_d = 1.52.

The bundle is covered with latex rubber tubing, which in turn is covered with tinned copper tubular braid. The ends are cemented into special slit blocks.

6. Sidearm Mount

The sidearm mount, set on 1/4-in. aluminum plate and similar to the one used in the experimental work (Figures 3 and 4), uses a larger lens for more light-gathering power and greater magnification. This mount is not attached directly to the sidearm of the welding machine but to a plate that has already been fitted to a particular machine. The layout is shown in Figure 26.

The distance from the arc to the lens is 88 mm and from the lens to the aperture is 264 mm. This gives an effective magnification of 3x. The lens selected is a coated achromat with a diameter of 34 mm and a focal length of 66 mm. Thus with a 1-mm (0.040-in.) entrance slit theoretically an arc gap of 0.014 in. can be viewed. The effective aperture of the lens is approximately 33 mm because of the retaining ring in the holder, and at this distance it accepts a solid angle of 22°. The optical axis with the work metal is 15°. In our estimation the diameter distance and magnification values are the best optical compromise. If a larger lens had been used, a larger angle with the work metal would be required. Then the probe would be looking into more of the hot puddle instead of behind it. If the lens were moved closer to the arc, more fogging would result and a larger angle with the work metal would be required.

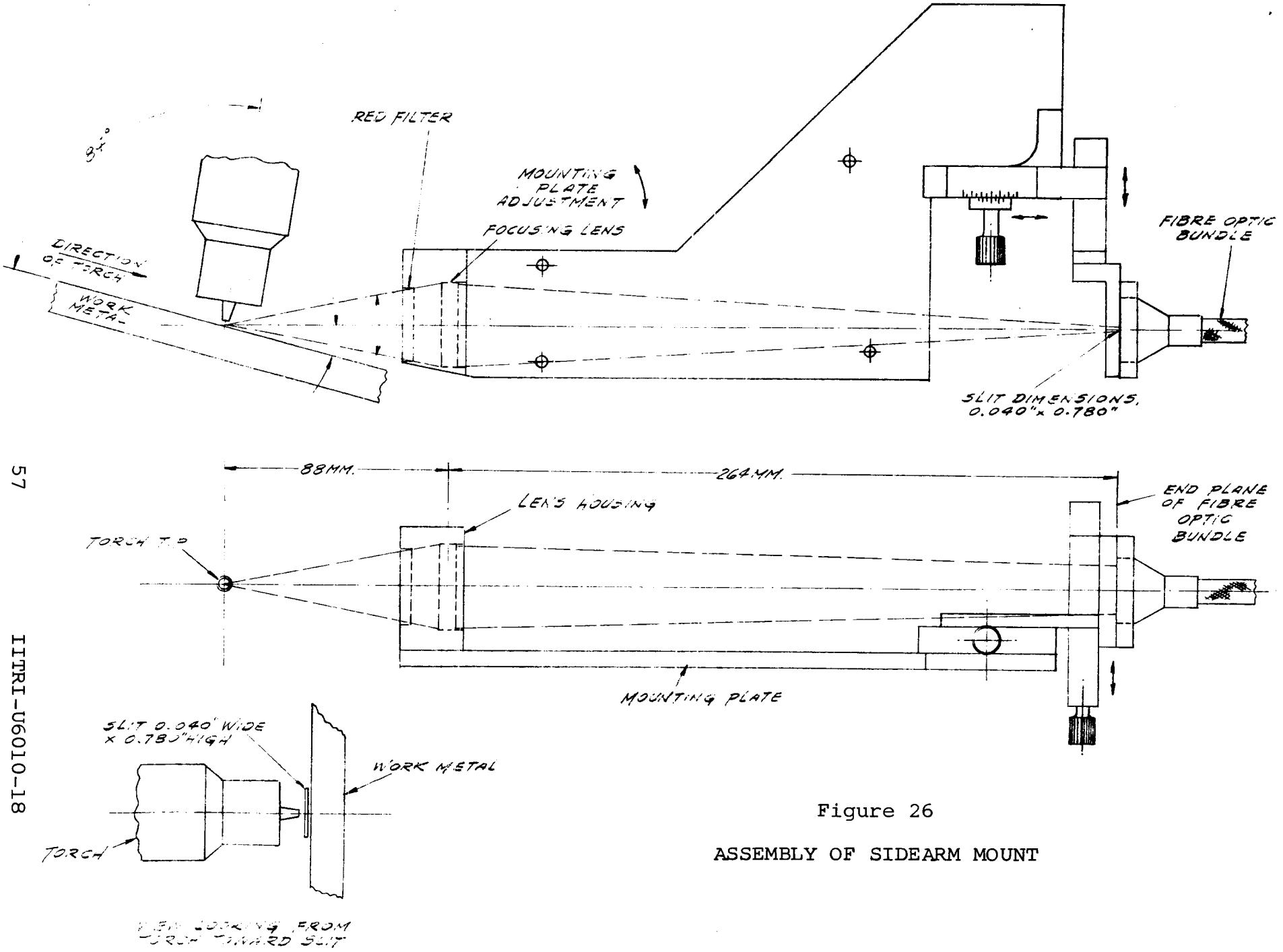

Figure 26

ASSEMBLY OF SIDEARM MOUNT

The light enters the fiber bundle at a solid angle of 7.5°, which is also the emerging angle at the entrance slit. This is sufficient to effectively fill the grating. This slightly overfills the grating, which is necessary to avoid variation of the background signal in a 5-cps pattern and thus to avoid recording a background signal as part of the AC signal. The aluminum block that holds the end of the fiber optic bundle also acts as the diaphragm on which the positions of the electrode tip and work metal can be observed. This diaphragm block is also mounted on the three-dimensional stage that permits the positions and focusing of any portion of the arc on the aperture.

A Kodak Wratten A series filter, which removes all spectra in the 2200- to 6000-A region, fits into the lens holder directly in front of the lens.

The overall optical layout is summarized in Figure 27.

B. Electronic System

1. Functional Description

The electronic system developed is essentially a three-channel system that monitors the hydrogen 6563 A line, the oxygen 7771 A line, and the argon 8521 A line. The last line is for the internal standard. The complete functional block diagram is shown in Figure 28. The instrument is operated completely from the 115VAC line. The AC feeds a synchronous chopper motor (5 rps), the regulated low-voltage DC supplies,

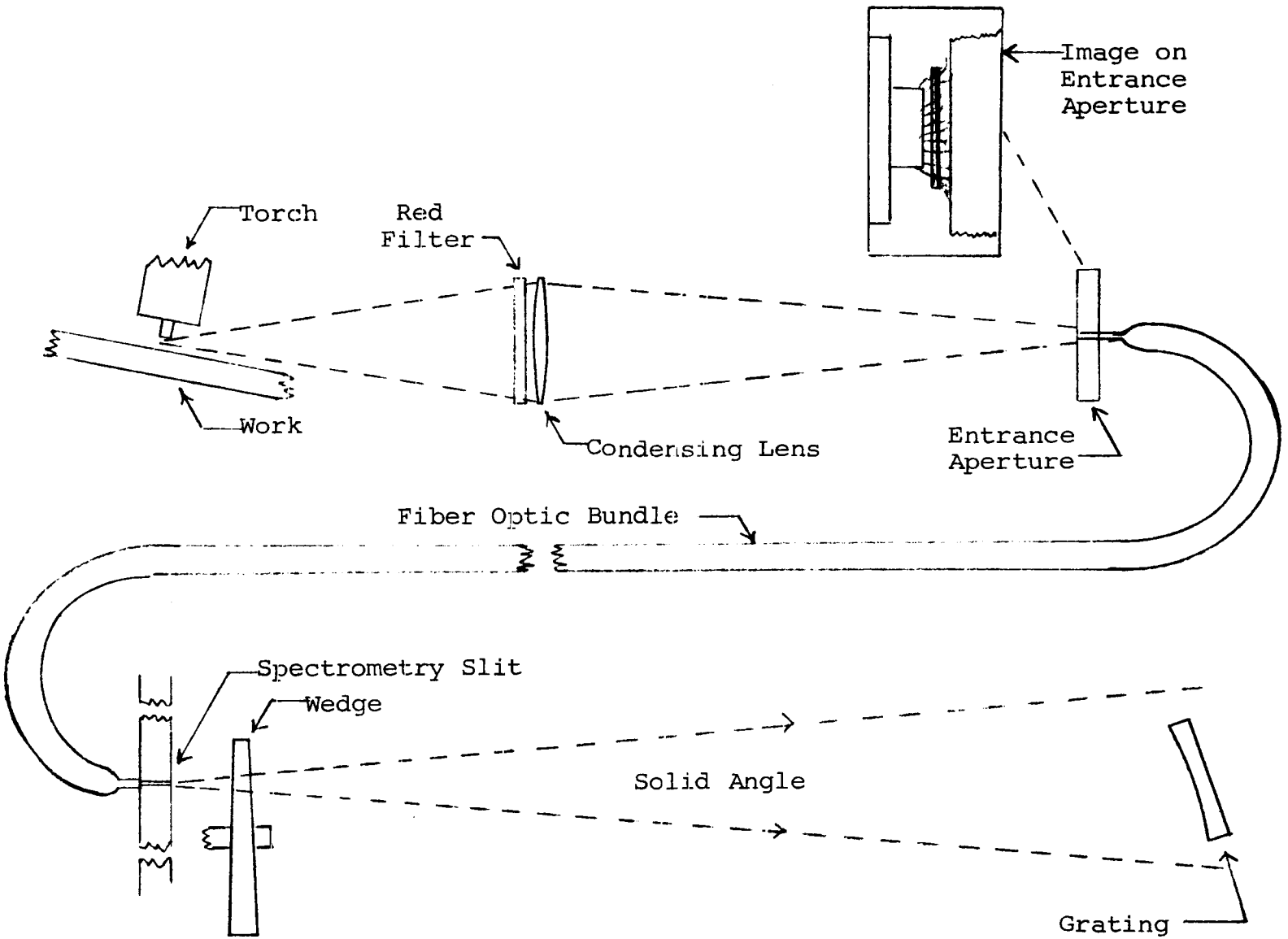

Figure 27

SUMMARY OF OVERALL OPTICAL LAYOUT

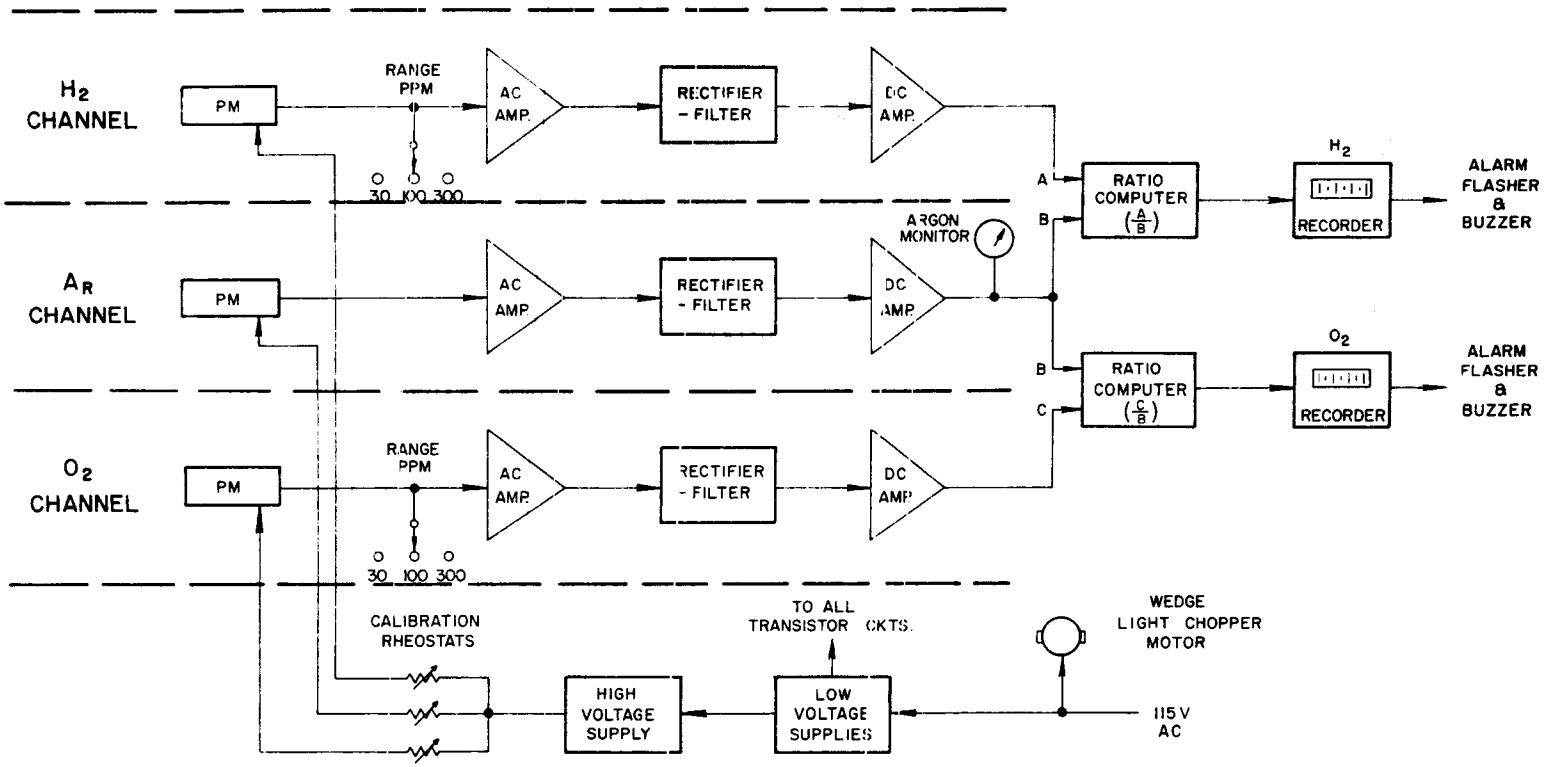

Figure 28

BLOCK DIAGRAM FOR WELDING SPECTROMETER READOUT

and some alarm circuitry, which is not shown. The low-voltage supplies, in turn, feed all of the amplifying and computing circuitry and the high-voltage regulated supply for the photomultiplier tubes. No vacuum tubes are used, except the two in the recorders themselves. Note that the individual calibration rheostats operate from the common high-voltage supply. The variation in system sensitivity (30, 100, and 300 ppm) is attained via a load-switching circuit at the output of the hydrogen and oxygen channels. The 10-cps signals from the three photomultipliers are then amplified via three AC-coupled amplifiers.

Behind the AC amplifiers are full-wave rectifiers, accomplishing nonsynchronous detection. These are followed by single time-constant filters. Amplification of the resulting DC signal levels is accomplished with small operational amplifier modules; the DC is thus raised to a voltage and power level applicable to operation of the Devar multiplier-divider computer modules, continuously computing the output ratio of each analytical line to the argon internal standard line. The quotient signals are finally applied to miniature point-tracking Rustrak recorders. The recorders have built-in adjustable high-level control contacts that operate in conjunction with separate control circuitry to form a high-level visual and audible alarm system.

2. Description of Components

a. The Photomultiplier and its Power Supply

The photomultiplier circuit is shown in the circuit diagram of a typical channel amplifier in Figure 29, and its power supply is shown in the circuit diagram of the control unit in Figure 30. The RCA type 7102 is a 10-stage end-cathode type with an S-1 spectral response. In this circuit it is operated at a nominal voltage of 1,000V with adjustments from 800 to 1,200V. A single Dumont-type Mu-metal shield is used to isolate the tube from magnetic fields. The dynode divider current of 100 μamp is sufficient to prevent appreciable loading due to either signal currents or excessive dark current. The range for each of the two analytical channels (0-30, 0-100, or 0-300 ppm) is changed by switching in different photomultiplier load resistances. Since the photomultiplier is a current-generating (high impedance) device, the output voltage is directly proportional to the load resistance. The full-scale anode voltage for each range is a nominal 0.8V peak-to-peak. Therefore the maximum signal current, which occurs in the 300-ppm position, is 0.8V/1.0M, or 0.8 μamp. For the argon channel a constant 10M load resistance is used.

The high voltage for the photomultipliers is obtained from a DC-DC converter (Figure 30); this is a solid-state module No. IL2-1750, supplied by the ITT Industrial Laboratory that generates 2,000VDC from a 28VDC input. The 28V input is derived from the +10V regulated supply (another module

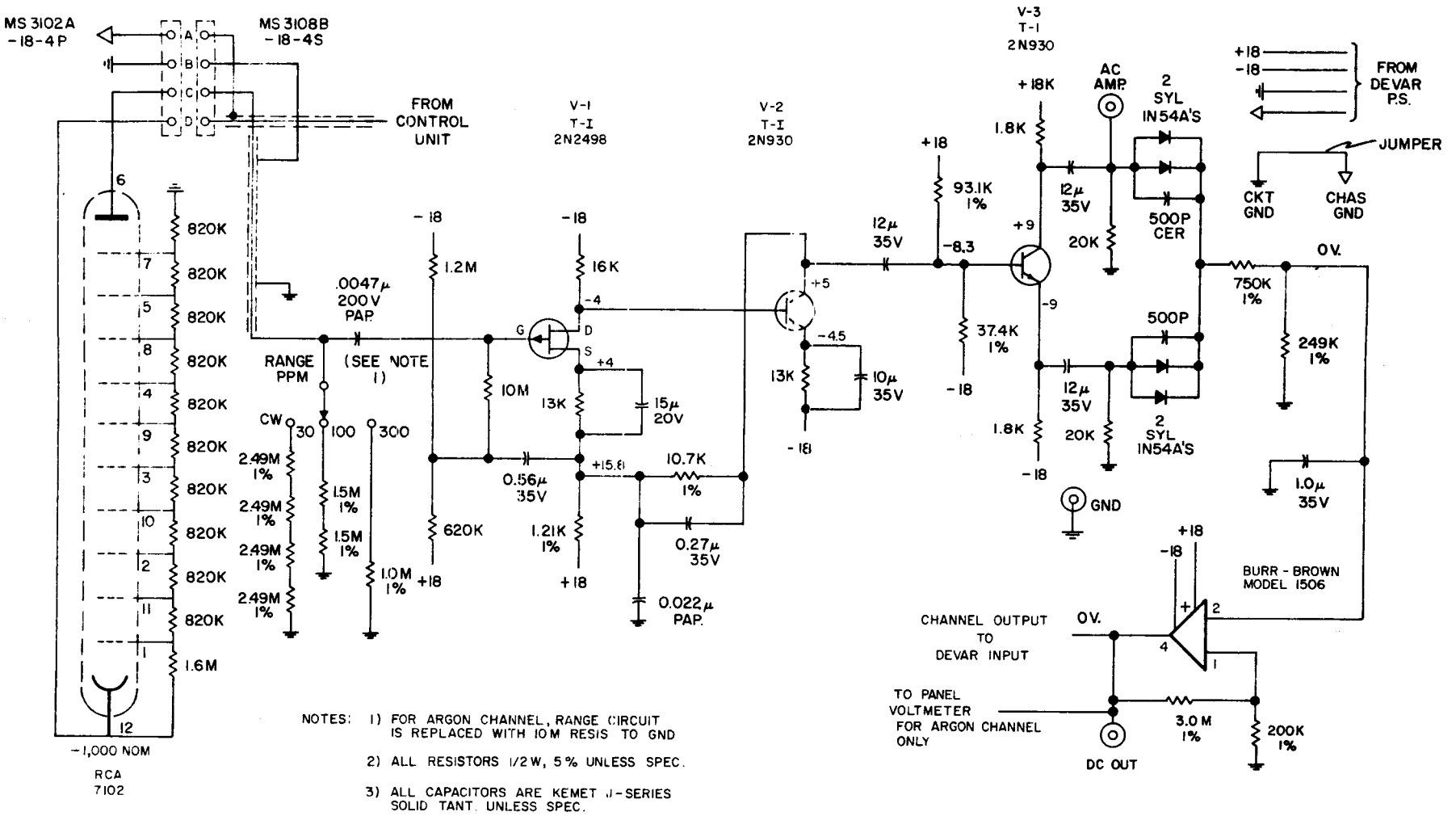

NOTES: 1) FOR ARGON CHANNEL, RANGE CIRCUIT IS REPLACED WITH 10M RESIS TO GND

2) ALL RESISTORS 1/2W, 5% UNLESS SPEC.

3) ALL CAPACITORS ARE KEMET J-SERIES SOLID TANT. UNLESS SPEC.

Figure 29

CIRCUIT DIAGRAM OF TYPICAL CHANNEL AMPLIFIER

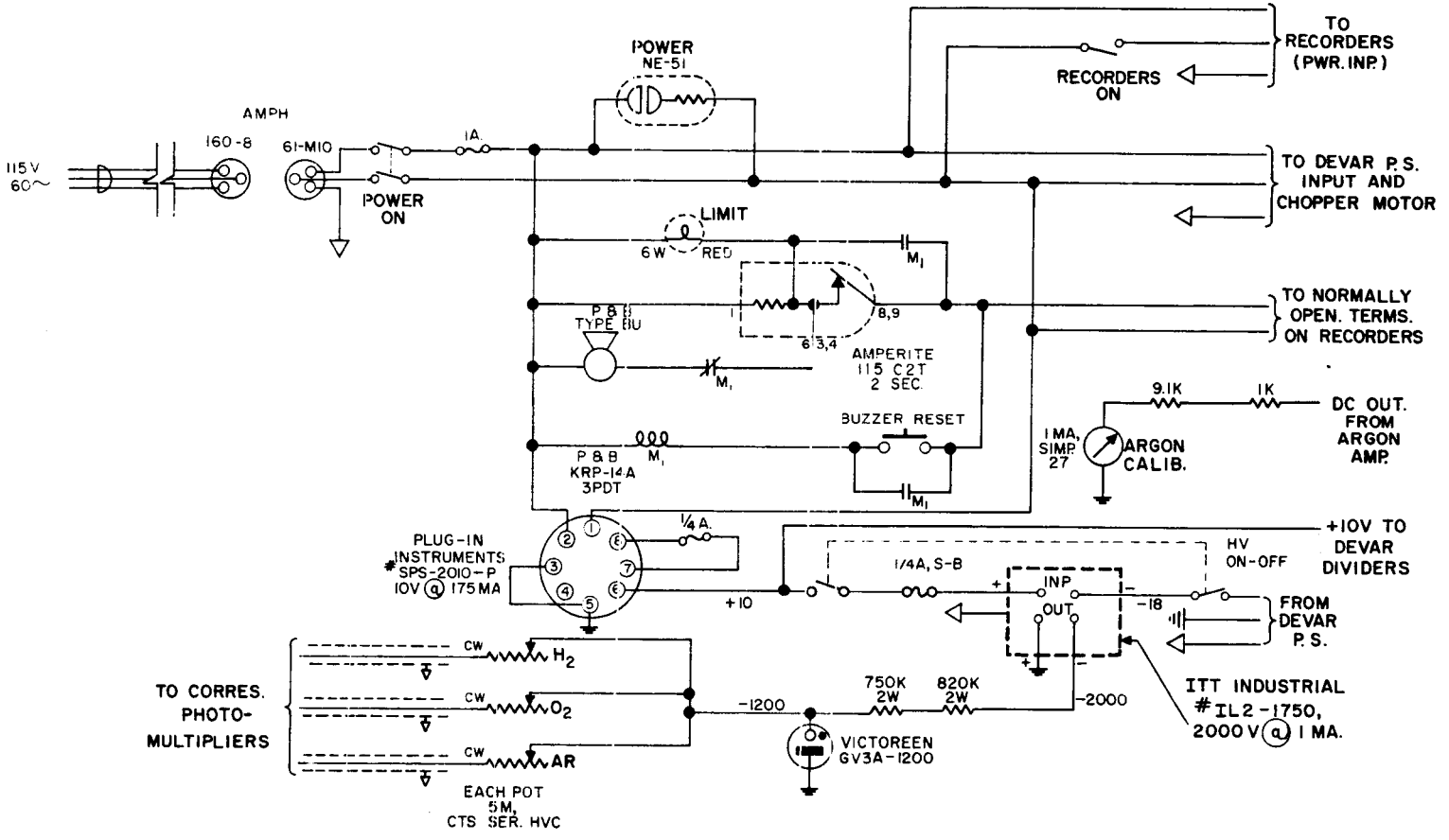

Figure 30

CIRCUIT DIAGRAM OF CONTROL UNIT

in the control unit) and the -18V from the Devar regulated power supply. The connections to this supply are shown in Figure 28. The -2,000V from the converter is applied to a corona-type regulator tube circuit; the corona tube operates at 1,200V. Individual rheostats for the three channels connected from the -1,200V line adjust the voltages across the photomultiplier dynodes to vary the gain of these tubes. This is an internal adjustment and should not have to be changed after the initial calibration of the various channels.

The effect of ambient temperature on the sensitivity of the photomultipliers results only from a change in photomultiplier supply voltage. With a 40°C temperature change, from 5°C to 45°C, the output voltage from the converter changes 4%. This changes the corona tube voltage 0.4% and, due to the eight power exponential relationship of the photomultiplier, changes the gain of the photomultiplier about 3%.

b. Channel Amplifier Circuitry

The three channel amplifiers, which are effectively carrier-type amplifiers, amplify the 10-cps signal from the respective photomultipliers, rectify, filter, and amplify the resulting DC signal for application to the multiplier-divider modules. As shown in Figure 28, a field-effect transistor is applied as a high-impedance input stage and is followed by a planar bipolar transistor for additional amplification. The third (bipolar) stage acts as a phase-splitter; two signals that differ in phase by 180° are produced and applied to a

full-wave rectifier circuit. Note that the second stage is directly coupled to the first and that a direct-coupled degenerative feedback loop exists between the two.

The open-loop voltage gain for the two stages is approximately 1,300 and the closed-loop gain is 10, giving a feedback factor of 43 decibels. The 10M bias return resistor at the field-effect transistor gate is bootstrapped to the source through the 0.56-μ coupling capacitor. This achieves an effective input impedance for the stage of 1,000M and thus presents a negligible load to the (maximum of) 10M photomultiplier load resistance.

The frequency response of the AC amplifier, as fed from a high-impedance source, is from 4 to 40 cps. The maximum signal output is 15 to 16V, peak-to-peak. This results in a DC signal at the filter output, taken across the 10-μ capacitor, of 0.64V. The rectifier-filter circuit is average reading and employs parallel-connected diodes and a high resistance load to achieve linearity over a wide range of signals. The filter time constant is approximately 0.2 sec.

The DC amplifier is a differential-input operational amplifier type. It is a small solid-state module mounted on the carrier amplifier circuit board along with the other components. Its feedback loop gives a stabilized gain of 16, raising the 0.64V filter output to a full-scale output of 10V for each channel. The DC amplifier is operated in a noninverted

mode to give a very high closed-loop input impedance so that loading of the high-impedance rectifier circuit is prevented.

Note that the DC output of all three channel amplifiers is routed to the appropriate input of the Devar multiplier-dividers (ratio computers) in Figure 28. The output of the argon channel, in addition, is routed to a panel meter circuit in the control unit. The meter circuit is arranged such that the full 10V for the channel reads full scale on the panel meter. The panel meter deflection is used in initial calibration of the system. This procedure is described later.

c. Ratio Computers

The two ratio computers are the Devar-Kinetics type 19-302 multiplier-divider. These are solid-state high-speed switching modules in which the computer functions are performed by varying the width and height of short pulses and by subsequent integration. The computer function is as follows.

$$X_0 = \left(\frac{A_1 X_1}{X_3} X_2 \right) A_0$$

where

A_1 and A_0 are constants

The principal constraints are:

$$\frac{A_1 X_1}{X_3} < 1$$

where

X_2 = positive polarity value

X_3 = positive polarity value.

In the present system, a +10V potential from the regulated supply in the control unit is used for X_2. Also, 40,000 ohm multiplying resistors are used for each of the A_1 and A_0 positions, making these constants 0.5 and 2, respectively. Thus the function becomes:

$$X_0 = \left(\frac{0.5\ X_1}{X_3}\ 10 \right)\ 2$$

Therefore if X_1, the analytical line signal energy, and X_3, the standard argon signal, are equal, the output for the Devars is actually 10V and the full-scale rated values for the X_1 and X_3 Devar inputs are also 10V. If for some reason the X_1 input should be greater than the X_3 input, the output would rise above the full scale of 10V and could not be read on the recorder. Thus the first constraint above must always be maintained. The physical circuitry does not permit X_3 to become negative; thus all of the constraints are met. The computer modules operate over a wide range of inputs; at 2% of full-scale input the output error is only 1%.

d. Control Unit, Recorders, and Power Supplies

The circuitry for the control unit is shown in Figure 30. The high-voltage regulator and the argon calibration circuit have already been discussed. The +10V power supply is the Plug-In Instruments model SPS-2010-P and is rated at 10V and 175-mamp output. This supply regulates line changes from 100 to 130VAC within 0.01% and has a noise output of 0.8 mV.

The alarm circuitry (Figure 30) consists of the thermal delay relay, the conventional relay, buzzer, light, and push button. When the high-level limit for either analytical channel is reached, the delay relay, the buzzer, and the light are energized. After a 2-sec delay, the delay contact opens, deenergizing the buzzer, the light, and the delay heater. After the heater cools, the contacts close again and so on, giving on-off cycles of approximately 2 sec each.

The two recorders are Rustrak model 141-A recorder-controllers. These are meter-movement miniature recorders in which a clamping bar intermittently clamps the meter needle to the pressure-sensitive paper, making a small dot. The clamping (striking) rate is 3-3/4 per sec and the chart speed is 450 in./hr, producing dots that are spaced 0.03 in. apart. Adjustable contacts are provided for high-level and low-level control. Only the high-level control is used in this system. When the meter needle reaches the point at which the contact is set, a ground circuit is completed and, through amplification, a control relay is energized. The circuit diagram for the recorder-control is shown in Figure 31.

The +18V and -18V sources, which feed the channel amplifiers, the ratio computers, and the high-voltage converter, are supplied by the Devar-Kinetics type 19-601 power supply. This is a solid-state regulated supply that regulates line variations from 95 to 130VAC within 0.025%; its noise output is 1 mV.

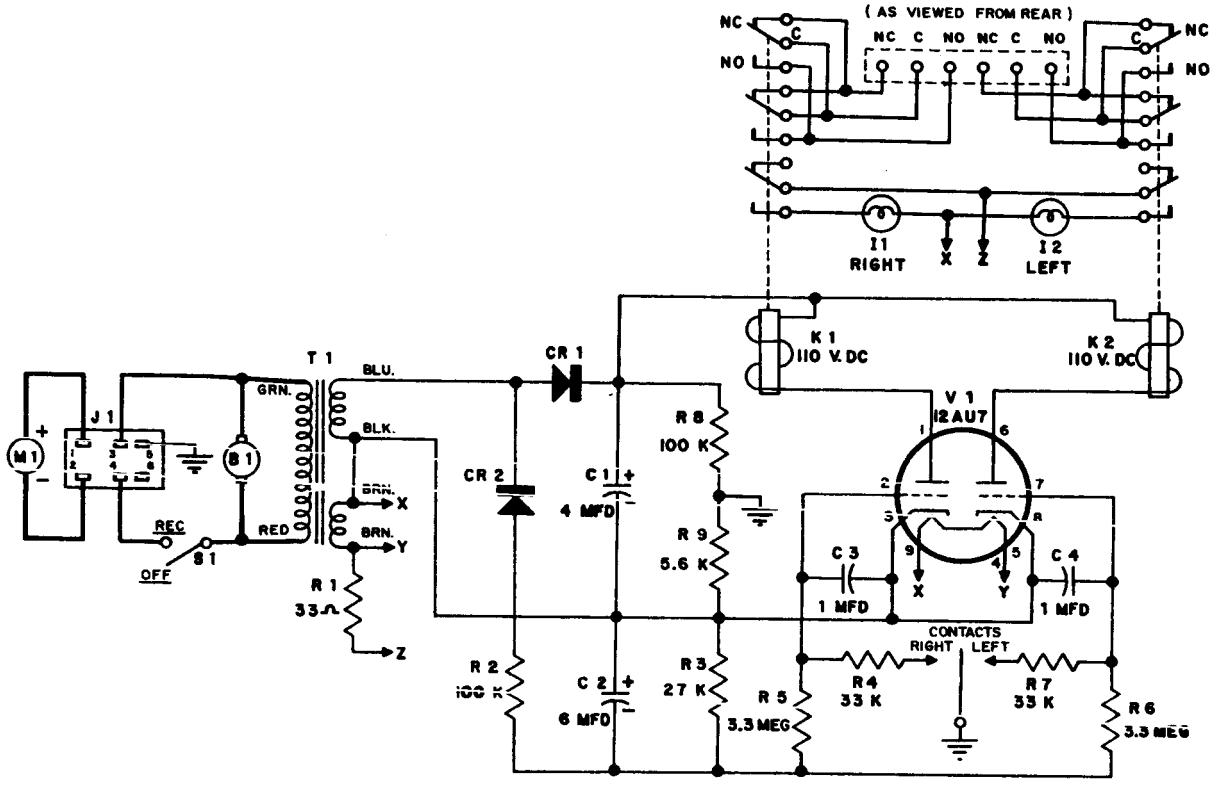

Figure 31

CIRCUIT DIAGRAM OF RUSTRAK RECORDER-CONTROLLER

e. Interconnecting Wiring

Figure 32 is the interconnecting wiring diagram. The various panel-mounted modules are arranged in the same physical locations as the actual modules. The connections to the three photomultipliers are located in the upper right with the military specifications connector pin designations. The wiring to the sychronous 300-rpm chopper motor is shown in the upper left. The +18V, -18V, and ground connections to the channel amplifier and the ratio computers are made with individual leads that run to a terminal board at the Devar power supply source. This facilitates troubleshooting and lessens the possibility of cross-coupling between channels. Separate circuit-ground and chassis-ground systems are used. The connections shown to the ratio computers are in the same relative positions as the actual connections. The two recording meters and the one panel meter are actually 1-mamp full-scale meters and are connected with 10,000-ohm series resistance to obtain the 10V full-scale deflection.

3. Calibrating Procedure

The electronic calibrating procedure for the Welding Spectrometer Analyzer is quite simple. Before actual calibration, however, it is advisable to check the position of the three exit slits with the aid of an oscilloscope. With the vertical input to the scope connected to the AC AMP test jack and the ground test jack of a given channel amplifier, the corresponding slit is adjusted such that a 10 pulses/sec

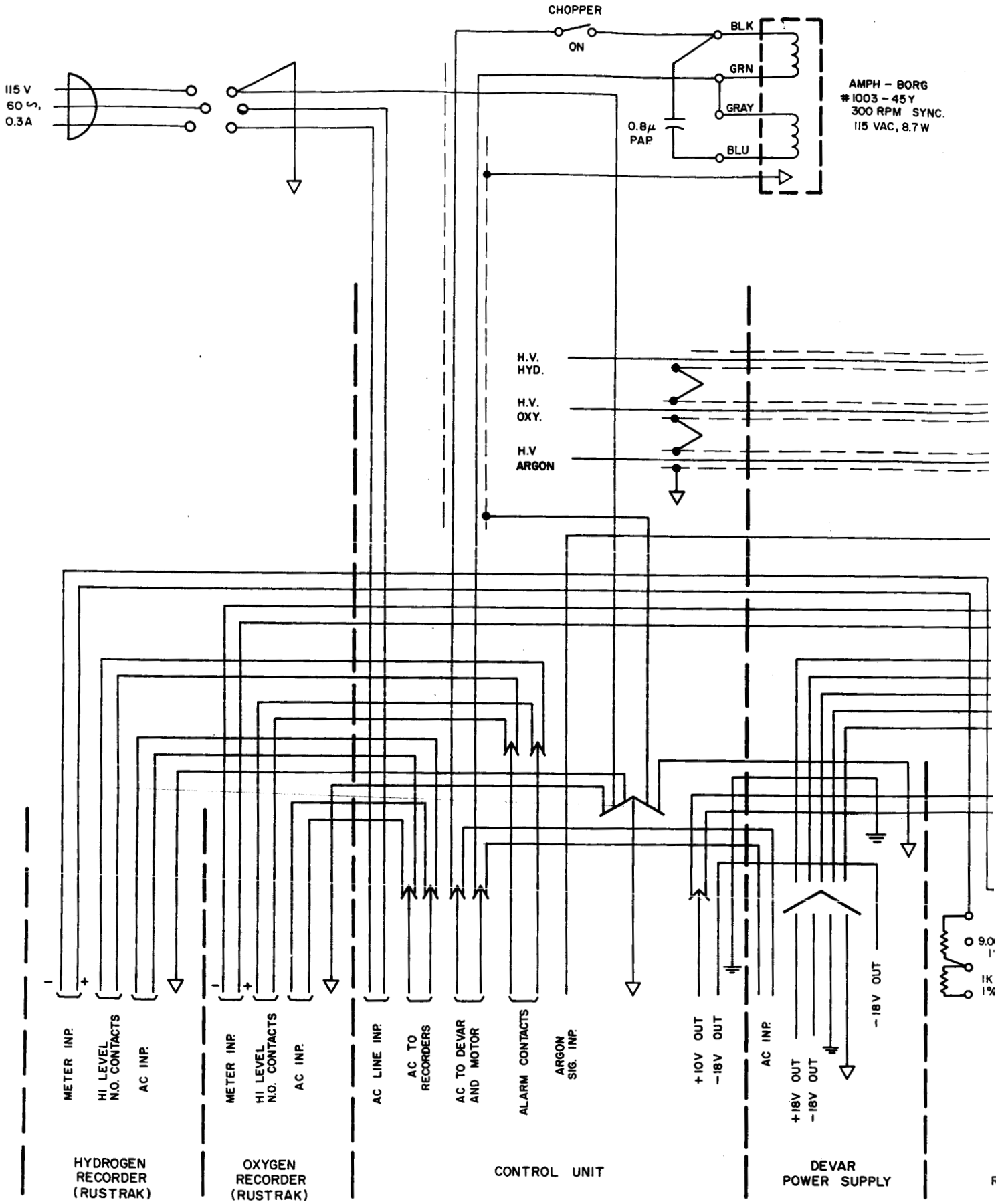

Fig 32

Figure

DIAGRAM OF INTERCONNECTING

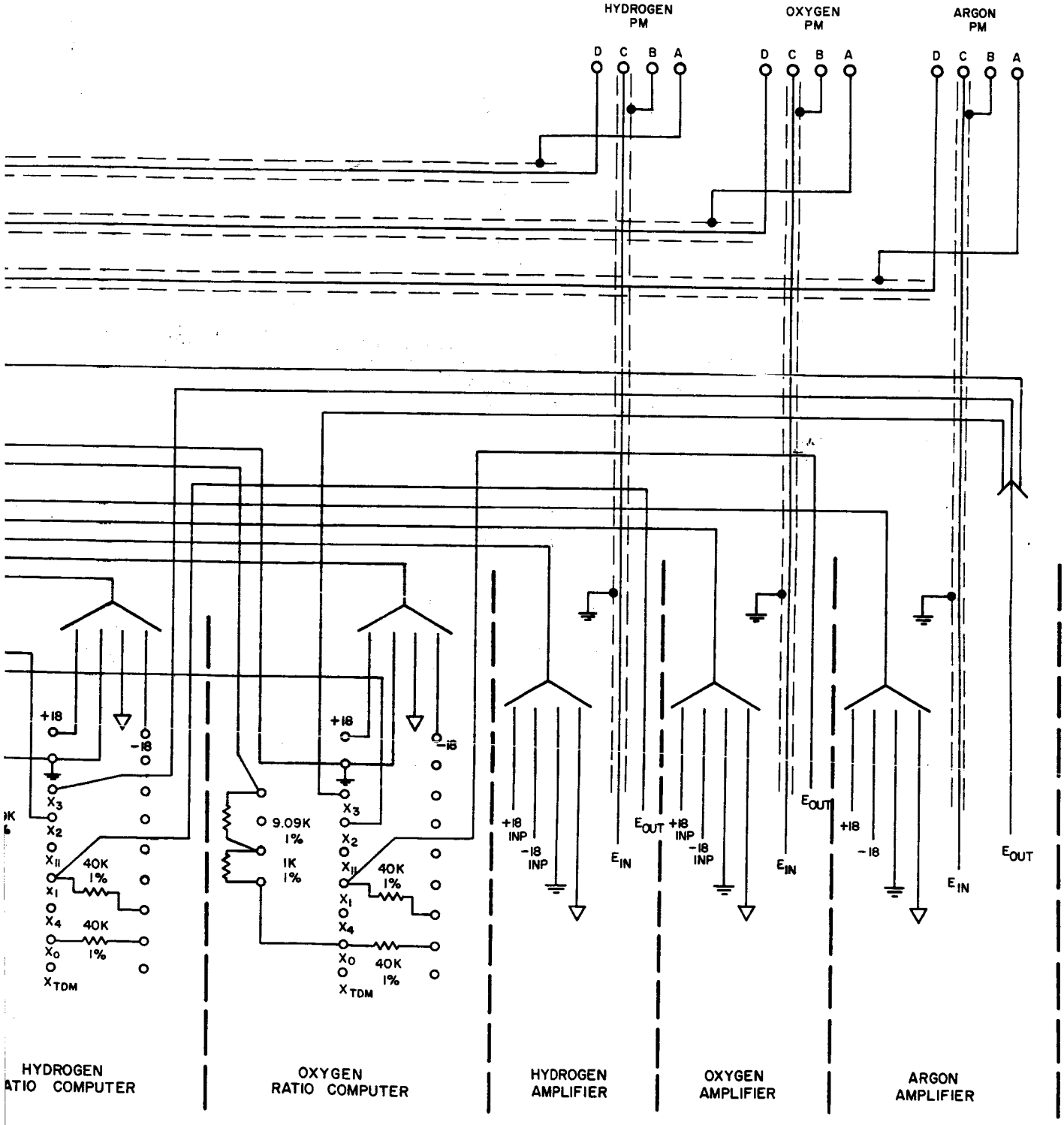

32

WIRING FOR INSTRUMENT

Fig 32 (2)

waveform is displayed. If the slit is sufficiently off center to one side or the other, only a 5 pulses/sec waveform would be obtained. The waveshape can be adjusted so that the duty cycle is not unduly high or low by adjusting the position of the wedge chopper.

In actual electronic calibration, the argon standard channel is set up first. With the predetermined percentage of argon added to the shield gas the rheostat inside the control unit labeled "AR" is adjusted so that an on-scale of the panel meter is obtained. The pot should then be locked. The hydrogen channel can next be calibrated. With a known concentration of hydrogen added to the shield gas, e.g., 100 or 200 ppm, the rheostat labeled "hydrogen" is adjusted so that the proper deflection is obtained on the hydrogen recorder (with the proper range selected at the channel amplifier). This pot should then be locked. The same procedure should be followed for the oxygen channel. The system now should be in proper calibration.

4. Operating Procedure

The operating procedure for the system is exceedingly simple. The instrument is turned on by means of the main power switch and the proper range selected for hydrogen and for oxygen at the respective channel amplifiers. During operation, the argon energy monitoring panel meter should be observed from time to time. It should not go off scale or to extremely low values for optimum accuracy. If the deflection does go to either extreme, a troubleshooting analysis must be made.

5. Troubleshooting Suggestions

All of the panel-mounted modules can be withdrawn from the cabinet and tested under power because of the slack lead length provided. If trouble is suspected in one of the channel amplifiers, check the DC voltages at the various points, as shown in the circuit diagram. If a channel appears to be noisy, connect an oscilloscope to the AC AMP jack. The noise at this point (with the unit in the rack or shielded with a sheet of grounded foil) should be less than 5 to 15 mm peak-to-peak of 60-cps pickup with the HV switch (photomultiplier supply) in the control unit turned off. Some random (white) noise will be added with the HV turned on and the chopper motor turned off because of the dark current flowing in the photomultiplier.

To test the various circuit points in the HV supply, a 20,000 ohms/volt (or higher) meter should be used to prevent loading. The current drawn by each photomultiplier dynode divider is only about 100 μamp; this fact should be considered if or when dynode voltage measurements are made.